RelB deficiency in dendritic cells protects from autoimmune inflammation due to spontaneous accumulation of tissue Tregs

Nico Andreas[1, 2, 10], Maria Potthast[3, 10], Anna-Lena Geiselhöringer[3, 10], Garima Garg[4], Renske de Jong[3], Julia Riewaldt[5, 6], Dennis Russkamp[3], Marc Riemann[1], Jean-Philippe Girard[7], Simon Blank[3], Karsten Kretschmer[5], Carsten Schmidt-Weber[3, 8], Thomas Korn[4, 9], Falk Weih[1] and Caspar Ohnmacht[3]*.

[1]Research Group Immunology, Leibniz Institute on Aging – Fritz Lipman Institute (FLI), Jena, Germany
[2]Institute of Immunology, Jena University Hospital, Jena, Germany.
[3]Center of Allergy and Environment (ZAUM), Helmholtz Center and Technical University Munich, Munich, Germany
[4]Klinikum Rechts der Isar, Department of Neurology, Technical University of Munich, Munich, Germany.
[5]Molecular and Cellular Immunology/Immune Regulation, DFG-Center for Regenerative Therapies Dresden (CRTD), Center for Molecular and Cellular Bioengeneering (CMCB), Technical University Dresden.
[6]Current address: Cellex Patient treatment GmbH, Dresden, Germany.
[7]Institut de Pharmacologie et de Biologie Structurale (IPBS), Université de Toulouse, CNRS, UPS, Toulouse, France.
[8]Member of the German Center for Lung Disease (DZL).
[9]Munich Cluster for Systems Neurology (SyNergy), Munich, Germany.
[10]These authors contributed equally to this work.

Running title

RelB deficiency in DCs protects from autoimmune inflammation

*Corresponding Author:

Caspar Ohnmacht
ZAUM, HMGU, building 57, room 103
Ingolstaedter Landstr. 1, 85764 Neuherberg, Germany
Phone: +49 89 3187-2556, FAX: +49 89 3187-2540
E-mail: caspar.ohnmacht@helmholtz-muenchen.de

Abstract

Foxp3$^+$ regulatory T cells are well-known immune suppressor cells in various settings. Here we provide evidence that knockout of the *relB* gene in dendritic cells of C57BL/6 mice results in a spontaneous and systemic accumulation of Foxp3$^+$ T regulatory T cells (Tregs) partially at the expense of microbiota-reactive Tregs. Deletion of *nfkb2* does not fully recapitulate this phenotype indicating that alternative NF-κB activation via the RelB/p52 complex is not solely responsible for Treg accumulation. Deletion of RelB in dendritic cells further results in an impaired oral tolerance induction and a marked type 2 immune bias among accumulated Foxp3$^+$ Tregs reminiscent of a tissue Treg signature. Tissue Tregs were fully functional, expanded independently of IL-33 and led to an almost complete Treg-dependent protection from experimental autoimmune encephalomyelitis. Thus, we provide clear evidence that RelB-dependent pathways regulate the capacity of dendritic cells to quantitatively and qualitatively impact on Treg biology and constitute an attractive target for treatment of autoimmune diseases but may come at risk for reduced immune tolerance in the intestinal tract.

Key points

- RelB defiency in dendritic cells leads to accumulation of tissue Tregs
- Treg accumulation occurs independent of IL-33 and at the expense of oral tolerance
- Tissue Treg accumulation protects from experimental autoimmune encephalomyelitis

Kewords

Non-canonical NFκB pathway, RelB, dendritic cells, tissue Tregs, autoimmune inflammation, EAE

Introduction

Regulatory T cells (Tregs) expressing the master transcription factor Foxp3 have been described as key cells for the regulation of otherwise exaggerated and potentially fatal immune responses, both to foreign- and self-antigens. More recently, it became apparent that Tregs operate in different flavours depending on co-expression of master transcription factors, cytokine and chemokine receptors typically associated with other T helper cell subsets (1). For instance, Foxp3$^+$ Tregs co-expressing the retinoic acid–related orphan receptor gamma t (ROR(γt)) describe a population of Tregs in the intestinal lamina propria that is induced only by colonization with commensal bacteria (2, 3). Likewise, T-bet-expressing Tregs prevent severe Th1-dominated autoimmunity, possibly due to co-localization with T-bet$^+$ effector T cells (4, 5). Combined deletion of both T-bet and Gata3 in Tregs has been shown to result in a spontaneous autoimmune disorder while deletion of Gata3 alone prevents Treg stability under inflammatory conditions (6, 7). Typically, Tregs derived from non-lymphoid tissues such as skin or adipose tissue show a remarkable expression of genes previously associated to type 2 immunity including the receptor for IL-33 (*Il1rl1*) and *Gata3*, and have been termed tissue Tregs (8-10). Local Tregs have been shown to play a key role for tissue integrity because Treg-intrinsic defects can result in reduced tissue function upon damage (11, 12). Thus, type 2 immune-biased Tregs may exert a similar role as steady state innate type 2 immunity in tissue homeostasis and repair (13). However, little is known about the cell-extrinsic mechanisms that imprint a tissue Treg phenotype into T cells.

Antigen-presenting cells (APCs) and notably dendritic cells (DCs) are well-known for their capacity to initiate adaptive immune responses while their role for tissue homeostasis and immune tolerance has been recognized only in recent years. For instance, conditional ablation of DCs leads to aggravated autoimmunity in a murine model of multiple sclerosis termed experimental autoimmune encephalomyelitis (EAE) (14). Furthermore, DCs are able to regulate tissue-resident Tregs both during thymic differentiation and by local activation (15). Constitutive ablation of DCs did initially not reveal a major impairment of thymic-derived Treg development but leads to a potentially autoimmune myeloproliferative disorder due to a defect in central tolerance (16, 17). By contrast, the absence of DCs but not myeloid cells impairs the generation of ROR(γt)$^+$ Tregs and oral tolerance induction (2, 18). Thus, DCs have the capability to shape Treg biology in various settings.

Here, we propose that expression of the non-canonical NF-κB pathway member RelB but not NF-κB2 in DCs has a dominant role in limiting the accumulation of Tregs with a tissue Treg signature. By contrast, commensal-induced ROR(γt)$^+$ Tregs and induction of oral tolerance are reduced after ablation of RelB in DCs. We further show that such type 2 immune-biased Tregs are functional *in vitro* and *in vivo* and that accumulation of tissue Tregs is independent of non-hematopoietic IL-33 expression. Finally, mice lacking RelB expression in DCs show attenuated hypersensitivity reactions

and are almost resistant to induction of autoimmune inflammation in the central nervous system (CNS) in the EAE model. Thus, inactivation of the non−canonical NF-κB member RelB in DCs leads to an accumulation of tissue Tregs and alters the ratio between self− versus foreign−reactive Tregs with consequences for different disease entities.

Material and Methods

Mice

The following mouse strains were used: RelB$^{KO/KO}$ (19), NF-κB2$^{KO/KO}$ (20), IL-33-LacZ gene-trap (IL-33$^{Gt/Gt}$) knockouts (21) Foxp3.gfp knock-in (Foxp3^{tm1Kuch}) mice (22) intercrossed to MOG TCR-specific 2D2 (Tg(Tcra2D2,Tcrb2D2)^{1Kuc}, (23)) and OT-II mice (Tg(TcraTcrb)425Cbn) (24) with the congenic marker CD45.1 (B6.SJL-Ptprc^{a} Pepc^{b}) were used as organs donors for adoptive transfer experiments. Mice expressing a DC-specific Cre recombinase (Tg(Itgax-cre)$^{1-1Reiz}$) mice (25) were purchased at the Jackson Laboratories and crossed with mice carrying a loxP-flanked exon 4 of the *relb* gene (RelB$^{fl/fl}$) (19) to achieve deletion of *relB* in DCs (called RelB$^{\Delta DC}$ throughout the manuscript) or mice carrying a loxP-flanked exon 1 and 2 (NF-κB2$^{fl/fl}$) (26) to achieve deletion of *nfkb2* in DCs (called NF-κB2$^{\Delta DC}$ throughout the manuscript). RelB$^{fl/fl}$ mice were crossed to Foxp3-promotor-driven BAC transgenic Cre mice (27) to generate Treg-specific RelB deletion or to a Foxn1-driven Cre transgenic mouse line (28) to generate mTEC-specific RelB deletion (19). For cell sorting experiments, RelB$^{\Delta DC}$ were intercrossed to Foxp3^{tm1Flv} (29) reporter mice. Treg-deficient scurfy mice (Foxp3^{sf}, (30)) were used at an age of 6 days. Littermate controls were used whenever possible. All mouse strains were backcrossed to a C57BL/6 background for at least 10 generations unless otherwise stated. sST2 was injected three times per week at a dose of 100 µg in PBS intraperitoneally for a total of three weeks into adult mice. All animals were kept under SPF conditions. All interventions were performed in accordance with the European Convention for Animal Care and Use of Laboratory Animals and were approved by the local ethics committee and appropriate government authorities.

Induction of EAE

EAE was induced by injection of 200 µl of an emulsion containing 200 µg MOG_{35-55} peptide (MEVGWYRSPFSRVVHLYRNGK) and 500 µg Mycobacterium tuberculosis H37Ra (BD Difco) in Complete's Freunds Adjuvants (CFA) subcutaneously at the base of tail. On day 0 and day 2 after immunization, mice received 200 ng pertussis toxin (PTX, Sigma). Alternatively, EAE was induced using a kit from Hooke laboratories according to the manufacturer's instructions. Clinical signs of disease were monitored according to the following scheme: 1 = tail paralysis, score 2 = hind limb impairment, score 3 = hind limb paralysis, score 4 = front limb paralysis, score 5 = death. In case hind limb movement was strongly impaired, mice were provided with a HydroGel H20 and easy accessible wet food. For analysis of cytokine producing T cells at peak of disease, brains were pooled from two to six individual mice to obtain enough cells for restimulation. For spinal cord, sample of two to three mice were pooled after normalization to weight before restimulation. Restimulation was either performed with MOG_{35-55} or PMA/Ionomycin for four hours. For the last two hours, Brefeldin A was added to the restimulated cells. When indicated, Tregs were ablated by intraperitoneal injection of

500 µg anti-CD25 antibody (clone PC61; BioXCell) on days -5 and -3 prior to MOG_{35-55} immunization. For transfer experiments 2.5 x 10^6 sort-purified Foxp3/GFP$^-$2D2$^+$ T helper cells were injected intravenously 24 h prior to MOG_{35-55} immunization. The induction of MOG-specific 2D2$^+$Foxp3/GFP$^+$ Tregs was analyzed by flow cytometry at day 7 after MOG_{35-55} immunization in inguinal lymph nodes.

Rescue of scurfy mice

2 x 10^6 sort-purified CD4+ splenocytes from WT or $RelB^{DDC}$ mice were injected intraperitoneally into 3 to 6 days-old $Foxp3^{KO/KO}$ (Scurfy) mice. Non-treated Scurfy mice did not receive any cells. Survival and body weight were monitored for 60 days after cell transfer.

OT-II cell transfer and OVA feeding:

Naïve T cells from spleens and lymph nodes of OTII/CD45.1 mice were sort-purified or isolated by magnetic separation using a naïve CD4$^+$ T cell isolation kit (Miltenyi, Germany) and 0.5 x 10^6 naïve OT-II T cells were injected intravenously into WT and $Relb^{\Delta DC}$ recipients. Upon transfer mice were fed with 1.5 % OVA fraction V (Sigma-Aldrich) in drinking water *ad libidum* for 9 days before analysis.

Bone marrow chimeras

Recipient mice were lethally irradiated by a Co-60 source with two doses of 6 Gy four hours apart. Irradiated mice were reconstituted with 8 x 10^6 purified bone marrow cells of respective donors by intravenous injection. After reconstitution, mice received 0.25 mg/ml Enrofloxacin (Baytril ®, Bayer Vital GmbH) in drinking water for 3 weeks. Bone marrow chimeras were analyzed 10-12 weeks after reconstitution.

Production and use of soluble ST2

Soluble ST2 (sST2) cDNA (amino acids 1-337) was designed and ordered at Invitrogen Strings. 5µl DNA fragment (20ng/µl) were digested with NheI and XhoI and digested fragment was gel-purified using the GeneJET Gel extraction kit according to manufacturer's instructions. Purified fragments were ligated with dephosphorylated NheI and XhoI digested pcDNA3.1 using T4 DNA ligase (NEB). Competent XL10 gold cells were transformed with the ligation mix according to manufacturer's guidelines and plated on agar plates containing 100 µg/ml ampicillin. Selected colonies were picked and plasmids were isolated using the GeneJET plasmid prep mini kit and sequenced. Plasmids from a clone with the correct sequence were used to transfect Hek293 cells with Lipofectamine 3000 Reagent (Thermo). To generate stable cell lines, transfected cells were cultured in complete RPMI in presence of G418 for 4 weeks. Presence of sST2 in the supernatant was confirmed by western blot using a polyclonal goat anti-sST2 antibody (Abcam) and ELISA (R&D). For large-scale production of

soluble ST2, supernatant of sST2-producing cells was affinity purified via his tag using nickel columns (HisTrap excel). sST2 was further purified using size-exclusion chromatography (HiLoad 16/600 Superdex 75 pg).

Biological activity of sST2 was proven according to standard protocols. Briefly, murine splenocytes were cultured in the presence of activating CD3/CD28 antibodies in the presence of 10 ng/ml IL-33 (Preprotech). Addition of sST2 entirely suppressed the IL-33-induced production of IL-5 in a dose dependent manner (data not shown).

Preparation of CNS mononuclear cells

At the peak of EAE, mice were sacrificed and perfused immediately with 10 ml cold PBS through the left cardiac ventricle after opening the right ventricle. Brains and spinal cords were removed, cut into small pieces and digested for 45 min at 37°C in 2.5 mg/ml Collagenase D and 1 mg/ml DNase in DMEM. The digestion preparation was homogenised through a 70 µm cell strainer and centrifuged at 400 g for 10 min. The cell pellet was resuspended in 37 % Percoll and layered onto 70 % Percoll. Percoll gradient was run at 1800 g for 20 min without break and the interphase containing mononuclear cells was collected for further analysis**.**

Isolation of gut lamina propria cells:

Lamina propria of small intestine was prepared as described (2). Briefly, small intestine was flushed with PBS and Peyer's patches were removed. Intestines were cut longitudinally and incubated in 30 mM EDTA in PBS at pH 8.0 on ice for 30 minutes. Thereafter, tissues were vigorously washed in PBS repeatedly, minced into small pieces and digested in RPMI containing 25mM HEPES, 0.05 mg/ml collagenase D (Roche) and 10 µg/ml DNase I (Sigma-Aldrich) at 37°C for one hour with intermittent pipetting and replacement of digestion media. Collected supernatants were filtered through a 70 µm cell strainer and centrifuged at 500 g for 10 min. The cell pellet was resuspended in a 40% Percoll (GE Healthcare) solution and layered onto an 80% Percoll layer. The Percoll gradient was run at 1500 g at RT for 15 min. The interlayer containing lamina propria mononuclear cells was collected and washed prior to further analysis.

Flow cytometry and cell sorting

Single cell suspensions were prepared by digestion with collagenase D and DNase I, mechanical organs disruption or peritoneal lavage, incubated with Fc blocking antibody (BD) and stained with the corresponding antibodies on ice. Intracellular staining was performed using a Foxp3 fixation/permabilization kit (eBiosciences) according to the manufacturer's instructions. Lived/dead exclusion was routinely performed using a kit from Life Technologies and Tregs or T effector cells

were identified as single cells as Live/dead$^-$CD45$^+$CD3$^+$CD4$^+$Foxp3$^+$ or Live/dead$^-$CD45$^+$CD3$^+$CD4$^+$Foxp3$^-$ cell, respectively. cDCs were identified as Live/dead$^-$,CD45$^+$ cells expressing high levels of MHC-II and CD11c. Cell sorting was performed with an ARIA III cell sorter (BD) and cell purity was typically around 99%. For data analysis FlowJo V7.5.2 (Tree Star) software was used.

Treg suppression assay

MHC-II$^+$ CD11c^{high} DCs were isolated from spleens of control mice and co-cultured with CFSE-labelled CD4$^+$CD62L$^+$CD44^{low}naive T helper cells isolated from control spleens in presence of 1 µg/mL of soluble α-CD3 for 3 days in a 96 well-plate. If indicated, Tregs from control or RelB$^{\Delta DC}$ spleens were cocultured at a 1:2 ratio. Ratio of T cells to DCs was 5:1 with 1x10^5 T cells per well.

ELISA

Sandwich ELISA for total serum IgE was performed using a polyclonal sheep anti-mouse IgE (The Binding Site) for coating and biotinylated rat anti-mouse IgE (clone R35-118, BD Biosciences) for detection. After incubation with streptavidin-peroxidase (Calbiochem) tetramethylbenzidine (TMB; Fluka) was used according to the manufacturer's instructions and absorption was measured at 450 nm. IL-2 and IL-33 serum levels were measured with a multiplex assay (MSD) according to the manufacturer's instructions.

RNA_Seq analysis

Total RNA was extracted from sort-purified Tregs from RelB$^{\Delta DC}$Foxp3^{RFP} mice from indicated organs using a RNeasy Micro Kit (Qiagen). Complete cDNA was synthesized from 5 µl total RNA using the SmartScribe reverse transcriptase (Takara Bio) with a universally tailed poly-dT primer and a template switching oligo followed by amplification for 12 cycles with the Advantage 2 DNA Polymerase (Takara Bio). After ultrasonic shearing (Covaris LE220), amplified cDNA samples were subjected to standard Illumina fragment library preparation using the NEBnext Ultra DNA library preparation chemistry (New England Biolabs). In brief, cDNA fragments were end-repaired, A-tailed and ligated to indexed Illumina Truseq adapters. Resulting libraries were PCR-amplified for 15 cycles using universal primers, purified using XP beads (Beckman Coulter) and then quantified with the Fragment Analyzer. Final libraries were equimolarly pooled and subjected to 75-bp-single-end sequencing on the Illumina Nextseq 500 platform, resulting in ~27-47 mio reads. Reads were mapped to the mouse genome (version mm10) with GSNAP ((31); v2018-03-11)) and splice sites from Ensembl (version 81) as support. RNA-seq data quality was assessed with RNA-SeQC ((32); v1.1.8). Uniquely mapped reads served as input for obtaining gene counts with featureCounts ((33); v1.6.0)

and Ensembl gene annotations (version 81). Principle component analysis and visualisation was done in R using prcomp and ggplot functions. Normalization for library size and identification of differentially expressed genes was done with the R package DESeq2 ((34); v1.18.1). DESeq2 p-values were adjusted for multiple testing (Benjamini-Hochberg) and genes with an adjusted p-value < 0.1 were considered as differentially expressed.

Statistics

Data were analyzed by two-tailed student's t test analyzed unless otherwise stated using GraphPad Prism software. Bar diagrams show mean± SD unless otherwise stated. Mann-Whitney-U test and two-way ANOVA with Turkey's multiple correction test was used in EAE experiments as indicated. *P<0.05, **P<0.01, ***P<0.001

Results

NF-κB members alter Foxp3$^+$ regulatory T cells in a DC-specific manner

Complete knockout of the non-canonical NF-κB member RelB has been shown to result in severe T cell dependent autoimmune inflammation (35-37). In most cell types, RelB typically pairs with p52, a breakdown product of NF-κB2/p100, to mediate signalling via the so-called alternative NF-κB pathway. Therefore, we first addressed whether genetic deletion of RelB or the regulatory element of the p100/NF-κB2 precursor protein (20) alters systemic Treg homeostasis. Confirming earlier observations, RelB deficiency resulted in a drastic increase of Foxp3$^+$ Tregs in the spleen (Figure 1A). Surprisingly, bone marrow chimeras receiving p100-deficient bone marrow did not show any alteration in Foxp3$^+$ Tregs (Figure 1A). To investigate a potential role of RelB or NF-κB2 in DCs for Treg biology, we crossed mice with a floxed allele of the *relb* gene (19) or *nfkb2* gene (26) to mice expressing the *Cre* recombinase under control of a DC-specific promoter (25) hereafter called RelB$^{\Delta DC}$ or NF-κB2$^{\Delta DC}$ mice, respectively. We first checked deletion efficacy in different cellular subsets of the spleen and bone marrow-derived macrophages (BMDM). As expected, splenic DCs showed the most efficient *relB* deletion (Figure S1A) compared to other splenic subsets. BMDMs also partially deleted RelB (Figure S1A) indicating at least modest expression of CD11c and recombination in other myeloid lineages. Still, in this manuscript we will continue to talk about DCs for consistency with the current literature related to Itgax-Cre line. Interestingly, RelB$^{\Delta DC}$ mice showed a similar increase in splenic Tregs as complete RelB-deficient mice while NF-κB2$^{\Delta DC}$ mice showed only a modest yet significant increase in Treg numbers (Figure 1B). In order to definitively exclude a Treg-intrinsic role of RelB, we additionally ablated RelB exclusively in Foxp3$^+$ Tregs. We did not find any difference in Treg numbers of mice lacking RelB in Foxp3$^+$ cells (Figure 1B) in line with recent findings for a T cell-extrinsic role of RelB in the regulation of Treg biology (38, 39). As both canonical and non-canonical NF-κB pathways regulate DC activation and maturation in an interactive manner (40) we addressed how splenic DCs are altered in the absence of RelB or NF-κB2. Conditional ablation of RelB but not NF-κB2 resulted in a slight reduction of overall DC frequencies and a relative increase of Sirpα$^-$CD8α$^+$ DCs that expressed high levels of DEC-205 (Figure 1C, D). This confirms earlier results in which RelB has been shown to be necessary for the development of splenic myeloid-related CD8α$^-$ DCs (cDC2s) (41-43). DEC-205 has been previously associated to Treg induction and the relative increase of DEC-205$^+$ DCs in RelB$^{\Delta DC}$ but not in NF-κB2$^{\Delta DC}$ mice may contribute to Treg accumulation (Figure 1C, D and (44). Besides DEC-205, altered expression patterns of co-stimulatory molecules on DCs may contribute to Treg accumulation in RelB$^{\Delta DC}$ mice. Indeed, DCs from RelB$^{\Delta DC}$ expressed less PD-L1 but more PD-L2 while expression of OX40L remained unchanged relative to control animals at steady state (Figure 1E). Thus, signalling via the NF-κB member RelB but not NF-κB2/p52 in DCs has a dominant role in controlling Treg homeostasis.

Enhanced differentiation of Tregs in the thymus could alternatively account for an accumulation of peripheral Tregs. Indeed, we found more Foxp3$^+$ Tregs in the thymus of adult RelB$^{\Delta DC}$ mice (Figure 1F). We also observed a slight reduction of thymic Sirpα$^+$ DCs in RelB$^{\Delta DC}$ but not NF-κB2$^{\Delta DC}$ mice similar to splenic DCs lacking RelB (Figure S1B and (42, 43)). Given that migration of peripheral Sirpα$^+$CD8^{lo} DCs to the thymus has been proposed to efficiently induce Treg differentiation (45, 46) the observed reduction of this DC subset in the thymus of RelB$^{\Delta DC}$ mice makes it unlikely that peripheral DCs contribute to thymic Treg accumulation. In line with decreased Treg frequencies in RelB$^{\Delta TEC}$ mice (19), simultaneous ablation of RelB in DCs and mTECs prevented increased Treg frequencies in the thymus of adult mice compared to control mice while Treg numbers in spleen were still increased (Figure 1F). Treg accumulation in spleens of RelB$^{\Delta DC\Delta TEC}$ mice may be due to altered negative selection in RelB$^{\Delta TEC}$ mice resulting in autoimmunity (19) and a dominant effect of RelB-deficient DCs in the periphery. As peripherally induced Tregs can migrate to the adult thymus (47), we measured Treg frequencies in very young mice, in which peripheral Treg conversion is still very limited. However, we did not observe an increase in thymic Treg frequencies at one or two weeks of age (Figure 1G). Finally, conversion of otherwise negatively selected T cells into the Treg lineage can equally result in enhanced Treg differentiation in the adult thymus. To test this hypothesis, we crossed RelB$^{\Delta DC}$ mice on a C57BL/6 background for one generation to a Balb/c background in which a superantigen encoding retrovirus is exclusively expressed in DCs (Mtv-6). This results in impaired negative selection of Vβ3$^+$ T cells in the constitutive absence of DCs (16). However, we did not find any difference among Vβ3$^+$ Tregs between C57BL/6 and mixed background mice in the absence of RelB in DCs (Figure S1C). In summary, these results indicate that accumulation of Tregs in RelB$^{\Delta DC}$ mice depends on age-dependent peripheral differentiation of Tregs by DC-intrinsic effects induced by the absence of RelB-dependent gene regulation.

Accumulated Tregs in RelB$^{\Delta DC}$ mice show a tissue Treg signature

As our results so far indicate an accumulation of Tregs by peripheral mechanisms we performed a detailed characterization of Tregs in several tissues of RelB$^{\Delta DC}$ and NF-κB2$^{\Delta DC}$ mice. All examined organs showed an accumulation of Foxp3$^+$ Tregs in RelB$^{\Delta DC}$ and RelB$^{KO/KO}$ mice and this was particularly pronounced among Helios$^+$ Tregs (Figure 2A and S2A and B and data not shown). This effect was almost completely blunted in NF-κB2$^{\Delta DC}$ mice (Figure 2A and S2A) indicating that Treg accumulation occurred in a RelB-dependent but NF-κB2-independent fashion. The high expression levels of Helios among accumulated Tregs in RelB$^{\Delta DC}$ and NF-κB2$^{\Delta DC}$ and mice argues for a preferential accumulation of Tregs specific for self-antigens because thymic and tissue-restricted neo-self-antigens have been shown to induce Tregs that express Helios (48, 49). As increased proliferation rates may contribute to Treg accumulation we measured intracellular Ki-67 expression among Tregs

of various organs. Indeed, we found higher Ki-67 expression in Tregs in spleen and lymph nodes but not thymus of RelB$^{\Delta DC}$ compared to control mice (Figure 2B).

In order to gain deeper insight into the identity of accumulated Tregs in RelB$^{\Delta DC}$ mice we performed RNA-seq analysis of sort-purified Tregs from RelB$^{\Delta DC}$ mice backcrossed to a Foxp3 reporter line. Indeed, Tregs derived from the peritoneal cavity (PEC) as one of the sites with the highest Treg accumulation revealed a number of differently expressed genes reminiscent of tissue Tregs in RelB$^{\Delta DC}$ mice including high expression levels of *Klrg1, Il1rl1, Gata3, Pparg, Itgae, Nrp1* and *Tnfrsf4* but low expression of *Bcl2* and *CCR7* (Figure 2C and S2C and (8)). We were able to confirm these Treg markers by flow cytometry including KLRG1, OX40 (encoded by *Tnfrsf4*), CD103, PD-1, ICOS, GITR and ST2 (encoded by *Il1rl1*) (Figure 2D and Figure S2D). Interestingly, some of the tissue Treg signature genes were even found to be differentially expressed in Tregs isolated from the spleen and thymus of RelB$^{\Delta DC}$ mice indicating a systemic shift in favour of tissue Tregs (Figure S2C). Expression of Satb1, a recently identified genome organizer necessary for proper Treg differentiation in the thymus upstream of Foxp3 expression (50), was expressed at lower levels in Tregs derived from RelB$^{\Delta DC}$ mice compared to controls in all organs (Figure 2C and Figure S2C).

Barrier organs such as the intestinal tract are exposed to both self- and harmless foreign antigens that similarly rely on induction of Foxp3^{+} Tregs for maintenance of immune tolerance. We confirmed that accumulated Tregs in RelB$^{\Delta DC}$ mice expressed higher Gata3 levels within the intestinal tract and this was again dominant among Helios^{+} Tregs (Figure 2E). Surprisingly, microbiota-induced ROR(γt)$^{+}$ Tregs in the small intestine were reduced in RelB$^{\Delta DC}$ mice (Figure 2F) even when excluding accumulated Helios^{+} Tregs (Figure S2E). As ROR(γt)$^{+}$ Tregs are able to regulate type 2 immunity (2) we tested whether a comparable phenotype was observed in T effector (Teff) cells of RelB$^{\Delta DC}$ mice. Indeed, Gata3^{+} Teff cells accumulated spontaneously in the intestinal tract of RelB$^{\Delta DC}$ mice (Figure 2G). Whether accumulation of Gata3^{+} Th2 cells is a direct consequence of RelB deficiency in DCs or a result of the altered Treg compartment remains to be addressed. In line with these observations we found elevated levels of IgE in the serum and on the surface of FcεRI-bearing basophils and mast cells of RelB$^{\Delta DC}$ mice, a hallmark of type 2 immunity (Figure 2H and Figure S3A and S3B). All of these observations could also be found in RelB$^{KO/KO}$ mice (Figure S3D-F) and (37). Despite this systemic type 2 immune bias in T cells and a tendency of increased blood eosinophils levels in RelB$^{\Delta DC}$ mice (Figure S3C) we did not find any visible signs of inflammation typically observed in RelB$^{KO/KO}$ mice (not shown and (35-37)). Thus, both RelB$^{KO/KO}$ and RelB$^{\Delta DC}$ mice show an accumulation of Gata3^{hi} tissue Tregs partially at the expense of ROR(γt) expressing Tregs.

Tissue Tregs in RelB$^{\Delta DC}$ mice accumulate independent of IL-33

In line with the systemic type 2 immune bias in T cells from RelB$^{\Delta DC}$ mice, we also observed higher expression of the IL-33 receptor ST2 on Gata3^{+} Teff cells and Helios^{+} Tregs (Figure 3A and B). Notably, ST2 expression has been previously linked to high Gata3 expression in Tregs (51). Given that IL-2/anti-IL-2 antibody complexes and particularly external IL-33 administration can boost the accumulation of ST2^{+} / Gata3^{+} Tregs (6, 51, 52), we asked whether excessive IL-2 or IL-33 could be one of the drivers for the accumulation of tissue Tregs in RelB$^{\Delta DC}$ mice (reviewed in (53)). First, we did not find differences in serum levels of IL-33 nor IL-2 in the serum of RelB$^{\Delta DC}$ mice compared to control mice (Figure 3C). In addition, blocking IL-33 by injection of a soluble ST2 (sST2) decoy receptor over 3 weeks did not reveal a major difference in total or ST2^{+} Treg frequencies (Figure 3D). As IL-33 is predominantly expressed by non-hematopoietic cells (21), we additionally created bone-marrow chimeras with IL-33$^{KO/KO}$ animals as recipients. Again, we found a similar increase in ST2^{+}Helios^{+} Tregs and Th2-biased Teff cells compared to wildtype recipients receiving bone marrow from RelB$^{\Delta DC}$ mice despite undetectable IL-33 levels in IL-33$^{KO/KO}$ recipients (Figure 3E). Noteworthy, constitutive IL-33-deficient mice possess normal levels of ST2^{+} Tregs (54). This may indicate that IL-33 expands Tregs to prevent tissue damage e.g. during on-going type 2 immune-driven inflammation but is not the primary driver for the tissue Treg phenotype under physiologic conditions or in RelB$^{\Delta DC}$ mice. Additionally, these results rule out a role of non-hematopoietic RelB expression e.g. by mTECs or other radio-resistant cells of non-hematopoietic origin (42).

In summary, these results reveal that the increase in Tregs with a tissue Treg phenotype is independent of IL-33 or other non-hematopoietic effects. Several RelB-dependent mechanisms in DCs may be in place that regulates Treg biology in an integrative manner depending on the antigenic source and/or the anatomical site.

Tregs from RelB$^{\Delta DC}$ mice are functional in vitro and in vivo

The type 2 immune bias of the accumulated Tregs observed in RelB$^{\Delta DC}$ mice raised the question whether these Tregs are still functional because Th2-reprogramming of Tregs after excessive IL-4 or IL-33 signalling and corresponding high Gata3 expression has been proposed to impair their tolerogenic function (52, 55). Therefore, we first co-cultured Tregs derived from RelB$^{\Delta DC}$ or control mice with Teff cells in the presence of wildtype myeloid DCs. Under these *in vitro* settings, we did not find a difference in their suppressive capacity (Figure 4A). Next, we tested whether Tregs from each genotype are able to prevent wasting disease in mice carrying the *scurfy* mutation that results in severe autoimmune inflammation due to an intrinsic Treg deficiency. When reconstituted with Tregs from RelB$^{\Delta DC}$ or control mice, scurfy mice could be rescued equally with only minor variations in survival and weight gain (Figure 4B). So far, these data indicate that Tregs from RelB$^{\Delta DC}$ mice are functional *in vitro* and *in vivo*. Finally, we also tested whether oral tolerance induction is enhanced in

RelB$^{\Delta DC}$ mice. We transferred congenically labelled naïve OT-II cells into RelB$^{\Delta DC}$ or control mice and applied ovalbumin via the drinking water. Surprisingly, we found reduced frequencies of *de novo* induced Tregs derived from naïve OT-II cells in RelB$^{\Delta DC}$ mice and these Tregs additionally expressed less ROR(γt) (Figure 4C). As we have previously shown that microbiota-induced ROR(γt)$^{+}$ Tregs are able to regulate Th2-dominated immune responses we also looked for *de novo* differentiation of Th2 cells (2). Indeed, we found an upregulation of Gata3 both within the Treg and the Teff cell compartment in RelB$^{\Delta DC}$ mice (Figure 4D and E). In summary, these results indicate that accumulated Tregs in RelB$^{\Delta DC}$ mice are functional and protect from inflammation. However, this occurs at the expense of impaired *de novo* Treg differentiation capacity and accumulating Th2 cells in the intestinal tract in response to foreign oral antigens similar to what has been found in germfree mice (56).

Accumulation of tissue Tregs protects from autoimmunity

Overall, our data indicate a specific accumulation of Tregs with a tissue Treg signature in RelB$^{\Delta DC}$ mice. Given that Gata3^{+} Tregs are still present in the absence of microbial stimulation by bacterial symbionts (2) we reasoned that most of the accumulated Tregs in RelB$^{\Delta DC}$ mice are specific for self-antigens and may thus protect from autoimmune inflammation. We therefore induced EAE in both RelB$^{\Delta DC}$ and control mice and followed disease scores. Intriguingly, RelB$^{\Delta DC}$ mice were almost completely protected from disease while littermates showed severe signs of autoimmune inflammation (max. mean score: 2.4 (control) vs. 0.58 (RelB$^{\Delta DC}$) (Figure 5A)). In line with the low EAE scores we found reduced absolute numbers of pathogenic cytokine-producing T cells in the spinal cord (Figure 5B and Figure S4A). Moreover, less of these infiltrating T cells were specific for MOG protein because restimulation with MOG$_{35-55}$ peptide revealed reduced numbers of CD154^{+} antigen-specific T cells in the CNS of RelB$^{\Delta DC}$ mice (Figure S4B). We also found more Gata3^{+} T and Treg cells in the CNS at the peak of the disease (Figure 5C and Figure S4C and D) and as expected increased numbers of Helios^{+} Tregs expressing ST2 (Figure 5D).

Next, we wanted to exclude a potential DC-intrinsic defect during the priming phase in the absence of RelB and therefore adopted a protocol of antibody-mediated depletion of Tregs prior to EAE induction (57). As expected, Treg depletion aggravated disease scores in control animals (Figure 5E). Despite the only moderate Treg depletion efficiency in RelB$^{\Delta DC}$ mice at the time of immunization and rapid Treg recovery at the peak of disease (Figure S4F and G) we observed similar disease scores in Treg-depleted RelB$^{\Delta DC}$ and control animals (Figure 5E). This was again associated with an accumulation of pathogenic cytokine-producing T effector cells in the CNS (Figure 5F). Thus, RelB-deficient DCs are capable of inducing a full-blown pathogenic immune response in the absence of an excess of polyclonal tissue Tregs. Notably, treatment of mice with recombinant IL-33, which is known to boost accumulation of tissue Tregs, is equally able to reduce EAE disease scores (58). In order to

address whether RelB$^{\Delta DC}$ mice support increased *de novo* production of self-reactive Tregs during EAE *in vivo* we transferred sort-purified MOG-specific 2D2Foxp3^{-} naïve T cells into RelB$^{\Delta DC}$ or control mice prior to EAE induction. Interestingly, 2D2 T cells started to upregulate Foxp3 in RelB$^{\Delta DC}$ but not control mice by day 7 after immunization in the draining inguinal lymph node before any sign of disease onset (Figure 5G). In summary, these data reveal a key role of tissue Tregs for preventing autoimmune inflammation which can be achieved through selected deletion of the NF-κB family member RelB in DCs.

Discussion

Antigen-presenting cells and notably DCs have been known as initiator cells for the induction of immune responses to foreign antigens while their role for active tolerance induction with therapeutic potential has been recognized only at the beginning of this century (59). Particularly the mutual relationship between DCs and Tregs through increasing DC numbers and a simultaneous increase of Tregs indicates a critical role of DC-T cell interactions for dictating Treg populations (60). Treg homeostasis and function in the periphery is further dependent on continuous triggering of the T cell receptor by (auto-) antigens most likely constantly presented by DCs. Yet, this effect is independent from Treg hallmarks like Treg signature gene expression or the ability to use IL-2 but alters expression of a number of tissue Treg-associated genes including Helios and Gata3 (61, 62). Here we have identified one pathway within the DC compartment that limits the proliferation and therefore also accumulation of tissue Tregs: Ablation of RelB but not NF-κB2 within CD11c^{+} cells leads to a drastic increase in Treg numbers which predominantly show a tissue Treg phenotype. Most likely, the majority of such accumulated Helios^{+} Tregs in RelB$^{\Delta DC}$ mice are specific for self-antigens as both thymic and tissue-restricted neo-self antigens are able to induce Helios^{+} Tregs while Treg-specific Helios expression has not been described in Tregs with T cell receptor specificities for foreign antigens (48, 49). Thus, it remains possible that both enhanced generation of Tregs in the thymus and increased *de novo* generation in the periphery contribute to the increase in Tregs even though the latter possibility may be more relevant in RelB$^{\Delta DC}$ mice according to *de novo* Treg induction of 2D2 T cells (Figure 5F) and low expression of Satb1 and Bcl2. Accumulated Tregs in RelB$^{\Delta DC}$ mice show hallmarks of tissue Tregs including expression of ST2, Gata3 and Helios and are able to almost completely protect from autoimmune inflammation of the CNS. DCs have been previously associated with maintenance and induction of self-reactive Tregs. However Batf3-dependent CD8α^{+} DCs were dispensable for the induction of prostate-specific Tregs (15). In line with these results, RelB$^{\Delta DC}$ mice show a reduction mainly in Sirpα^{+}CD8α^{-} DCs but not CD8α^{+} (Batf3-dependent DCs) due to cell-intrinsic developmental defects in the absence of RelB (42, 43). This results in a dominant accumulation of DEC-205^{+} DCs that have been previously shown to be ideal targets for antigen-

specific tolerance applications via induction of Foxp3$^+$ Tregs (44). Notably, therapeutic targeting of MOG-expression to DCs was able to induce PD-1$^+$ Tregs and protect mice from EAE while conditional ablation of DCs resulted in a more severe Inflammation of the CNS (14).

Mechanistically, ST2-deficiency has been shown to prevent Gata3 expression in Tregs and exogenous IL-33 is able to induce accumulation of ST2$^+$ Tregs (8, 51, 63). However, accumulated tissue Tregs in RelB$^{\Delta DC}$ mice were independent from non-hematopoietic IL-33 and also neutralization of IL-33 by soluble ST2 did not reduce Treg levels significantly even though it remains possible that DCs themselves are able to provide IL-33 e.g. within the immunological synapse for expansion of type 2-biased Tregs in RelB$^{\Delta DC}$ mice that we were unable to neutralize (Figure 3 and (52, 64)). Noteworthy is that IL-33-deficient mice possess normal levels of ST2$^+$ Tregs (54). This may indicate that IL-33 expands Tregs to prevent tissue damage e.g. during on-going type 2 immune-driven inflammation but is not the primary driver for the tissue Treg phenotype under physiologic conditions. Alternatively, IL-2/anti-IL-2 antibody complexes are able to induce high numbers of Gata3-expressing Tregs and activation of T cells by RelB-deficient DCs has been shown to result in increased IL-2 production by T cells or DCs (6, 63, 65) but we did not find any difference in systemic IL-2 or IL-33 cytokine levels in the serum or peritoneal lavage of RelB$^{\Delta DC}$ mice.

In line with their assumed specificity for self-antigens, tissue Tregs have been shown to regulate a number of physiological processes including muscle repair, lung integrity after influenza infection and metabolic disorders in fat tissues (10-12). We now demonstrate that increasing tissue Treg numbers through ablation of DC-intrinsic RelB is also able to prevent autoimmune inflammation (Figure 5). Notably, treatment of mice with recombinant IL-33, which amongst other effects is known to boost accumulation of tissue Tregs, is able to equally reduce EAE disease scores (58). It remains to be addressed how tissue Tregs could fulfil this task but three general possibilities seem plausible: First, tissue Tregs could modulate DCs to prevent effective priming towards bona-fide self-antigens. This possibility has been proposed as a general concept for Treg function but could be dangerous for simultaneous immune responses of different origins and directed towards distinct specificities. Second, accumulation of tissue Tregs could enhance tissue integrity and prevent e.g. break of the blood-brain barrier as has been shown for other tissues like lung and muscle (11, 12). Finally, Tregs may prevent antigen-specific T cell responses directly. This would require expansion of *de novo*-induced Tregs (Figure 5G) or necessitate the accumulation of MOG-specific Tregs at steady sate in RelB$^{\Delta DC}$ mice. How RelB deficiency in DCs can result in enhanced *de novo* induction and accumulation of self-reactive Tregs but at the same time result in impaired *de novo* to orally supplied, foreign antigens remains to be identified but different functional programs exploited by different DC subsets adapted to their local environment and tissue function are likely in place.

Protection from autoimmune inflammation in RelB$^{\Delta DC}$ mice comes at a high cost as we have observed impaired tolerance induction in response to oral antigens and particularly in the numbers of ROR(γt)$^{+}$ Tregs. This Treg subset is now seen as a major factor for tolerance of symbiotic microbes and is essential for the efficient suppression of different forms of colitis (2, 3, 66, 67). Interestingly, RelB$^{\Delta DC}$ mice show a type 2 bias both within the Treg and the Teff compartment in PEC and small intestine and also after oral antigen exposure. This may be attributed due to cell-intrinsic defects in tissue-resident DCs but also to the lower numbers of ROR(γt)$^{+}$ Tregs counteracting type 2 immunity (2). Related to these results DC-specific ablation of TRAF6 – a key adaptor protein for the integration of TLR and some TNFR members into NFκB activation – leads to a spontaneous inflammation of the small intestine characterized by impaired Treg differentiation in response to oral antigen and a marked type 2 immune bias including accumulation of Th2 cells and eosinophils (68). TRAF6 can also signal via the classical NF-κB pathway but recent evidence suggests that NF-κB signalling in DCs can not be strictly divided into classical and alternative signalling pathways (40). Our observation that deletion of NF-κB2 in DCs did not fully recapitulate the deletion of RelB in DCs in terms of Treg accumulation (Figure 2A) supports the importance of RelB/p50 or complexes or NF-κB2 homodimers in DCs cross-regulation via classical NF-kB pathways.

Full knockout of RelB results in a fulminant autoimmune inflammation which is dependent on the adaptive immune system (37). However, this can be attributed to the essential role of RelB in mTECs and as a consequence impaired negative selection (19). Indeed, patients suffering from RelB deficiency have to undergo hematopoietic stem cell transplantation (HST) due to severe immune deficiency (69). Noteworthy is that at least in one case increased frequencies of Tregs were observed in a RelB-deficient patient before HST (personal communication to C.R.). Thus, increased Treg numbers cannot control autoimmune inflammation due to impaired central tolerance per se. The reasons for this observation may lay in potential differences and sources of respective self-antigens.

This observation supports our results that RelB could be an attractive target to enhance the number of tissue Tregs for the treatment of autoimmune diseases even though not at zero cost. Indeed, infusion of RelB-silenced DCs have been used to treat on-going myasthenia gravis and shown to prolong allograft tolerance, which was again associated with a Th2 and Treg bias (70-72). Likewise, transfer of wildtype DCs into RelB-deficient hosts has been shown to reverse airway inflammation and counteract the type 2 bias observed in these mice (73). Finally, type 2-biased Tregs have been found to accumulate in tumorigenic environments and may contribute to prevent effective anti-tumour immunity (74). Such ‘negative’ functions of type 2-immune biased Tregs may help to explain why the number of tissue Tregs is limited by RelB-dependent DCs. In summary, the inverse association of RelB-expressing DCs with the accumulation of Th2-biased tissue Tregs proves a dominant effect of tissue Treg numbers for effective protection from autoimmunity.

Acknowledgements

This work is dedicated to Falk Weih who regrettably departed from this life before the end of our study. We will always remember him as a passionate scientist, a wise group leader and first and foremost, a good friend. We thank Benjamin Schnautz and Johanna Grosch for technical assistance and Boris Reizis, Veit Buchholz, Dirk Baumjohann and Ursula Zimber-Strobl for providing mice.

Author contributions

N.A., M.P. and A.G., performed experiments and analysed data with the help of G.G., R.d.J., M.R. and C.O., D.R. produced sST2 and helped with experiments. J.R. and K.K. helped with *in vivo* experiments. J.-P. G. provided essential mouse strains. S.B., C.S.-W. and T.K. helped with specific analysis. F.W. initiated the study, N.A., M.P. and C.O. conceived the study and C.O. wrote the manuscript. All authors discussed and approved the manuscript.

Declaration of Interests

The authors declare no conflict of interest.

Data availabity

RNA-seq data have been deposited in NCBI's Gene Expression Omnibus through GEO Series accession number GSE134779 (https://www.ncbi.nlm.nih.gov/geo/query/acc.cgi?acc=GSE134779).

References

1. Josefowicz, S. Z., L. F. Lu, and A. Y. Rudensky. 2012. Regulatory T cells: mechanisms of differentiation and function. *Annu Rev Immunol* 30: 531-564.
2. Ohnmacht, C., J. H. Park, S. Cording, J. B. Wing, K. Atarashi, Y. Obata, V. Gaboriau-Routhiau, R. Marques, S. Dulauroy, M. Fedoseeva, M. Busslinger, N. Cerf-Bensussan, I. G. Boneca, D. Voehringer, K. Hase, K. Honda, S. Sakaguchi, and G. Eberl. 2015. MUCOSAL IMMUNOLOGY. The microbiota regulates type 2 immunity through RORgammat(+) T cells. *Science* 349: 989-993.
3. Sefik, E., N. Geva-Zatorsky, S. Oh, L. Konnikova, D. Zemmour, A. M. McGuire, D. Burzyn, A. Ortiz-Lopez, M. Lobera, J. Yang, S. Ghosh, A. Earl, S. B. Snapper, R. Jupp, D. Kasper, D. Mathis, and C. Benoist. 2015. MUCOSAL IMMUNOLOGY. Individual intestinal symbionts induce a distinct population of RORgamma(+) regulatory T cells. *Science* 349: 993-997.
4. Levine, A. G., A. Medoza, S. Hemmers, B. Moltedo, R. E. Niec, M. Schizas, B. E. Hoyos, E. V. Putintseva, A. Chaudhry, S. Dikiy, S. Fujisawa, D. M. Chudakov, P. M. Treuting, and A. Y. Rudensky. 2017. Stability and function of regulatory T cells expressing the transcription factor T-bet. *Nature* 546: 421-425.
5. Koch, M. A., G. Tucker-Heard, N. R. Perdue, J. R. Killebrew, K. B. Urdahl, and D. J. Campbell. 2009. The transcription factor T-bet controls regulatory T cell homeostasis and function during type 1 inflammation. *Nat Immunol* 10: 595-602.
6. Wohlfert, E. A., J. R. Grainger, N. Bouladoux, J. E. Konkel, G. Oldenhove, C. H. Ribeiro, J. A. Hall, R. Yagi, S. Naik, R. Bhairavabhotla, W. E. Paul, R. Bosselut, G. Wei, K. Zhao, M. Oukka, J. Zhu, and Y. Belkaid. 2011. GATA3 controls Foxp3(+) regulatory T cell fate during inflammation in mice. *J Clin Invest* 121: 4503-4515.
7. Yu, F., S. Sharma, J. Edwards, L. Feigenbaum, and J. Zhu. 2015. Dynamic expression of transcription factors T-bet and GATA-3 by regulatory T cells maintains immunotolerance. *Nat Immunol* 16: 197-206.
8. Delacher, M., C. D. Imbusch, D. Weichenhan, A. Breiling, A. Hotz-Wagenblatt, U. Trager, A. C. Hofer, D. Kagebein, Q. Wang, F. Frauhammer, J. P. Mallm, K. Bauer, C. Herrmann, P. A. Lang, B. Brors, C. Plass, and M. Feuerer. 2017. Genome-wide DNA-methylation landscape defines specialization of regulatory T cells in tissues. *Nat Immunol* 18: 1160-1172.
9. Panduro, M., C. Benoist, and D. Mathis. 2016. Tissue Tregs. *Annu Rev Immunol* 34: 609-633.
10. Vasanthakumar, A., K. Moro, A. Xin, Y. Liao, R. Gloury, S. Kawamoto, S. Fagarasan, L. A. Mielke, S. Afshar-Sterle, S. L. Masters, S. Nakae, H. Saito, J. M. Wentworth, P. Li, W. Liao, W. J. Leonard, G. K. Smyth, W. Shi, S. L. Nutt, S. Koyasu, and A. Kallies. 2015. The transcriptional regulators IRF4, BATF and IL-33 orchestrate development and maintenance of adipose tissue-resident regulatory T cells. *Nat Immunol* 16: 276-285.
11. Arpaia, N., J. A. Green, B. Moltedo, A. Arvey, S. Hemmers, S. Yuan, P. M. Treuting, and A. Y. Rudensky. 2015. A Distinct Function of Regulatory T Cells in Tissue Protection. *Cell* 162: 1078-1089.
12. Burzyn, D., W. Kuswanto, D. Kolodin, J. L. Shadrach, M. Cerletti, Y. Jang, E. Sefik, T. G. Tan, A. J. Wagers, C. Benoist, and D. Mathis. 2013. A special population of regulatory T cells potentiates muscle repair. *Cell* 155: 1282-1295.
13. Wynn, T. A. 2015. Type 2 cytokines: mechanisms and therapeutic strategies. *Nat Rev Immunol* 15: 271-282.
14. Yogev, N., F. Frommer, D. Lukas, K. Kautz-Neu, K. Karram, D. Ielo, E. von Stebut, H. C. Probst, M. van den Broek, D. Riethmacher, T. Birnberg, T. Blank, B. Reizis, T. Korn, H. Wiendl, S. Jung, M. Prinz, F. C. Kurschus, and A. Waisman. 2012. Dendritic cells ameliorate autoimmunity in the CNS by controlling the homeostasis of PD-1 receptor(+) regulatory T cells. *Immunity* 37: 264-275.
15. Leventhal, D. S., D. C. Gilmore, J. M. Berger, S. Nishi, V. Lee, S. Malchow, D. E. Kline, J. Kline, D. J. Vander Griend, H. Huang, N. D. Socci, and P. A. Savage. 2016. Dendritic Cells Coordinate the Development and Homeostasis of Organ-Specific Regulatory T Cells. *Immunity* 44: 847-859.
16. Ohnmacht, C., A. Pullner, S. B. King, I. Drexler, S. Meier, T. Brocker, and D. Voehringer. 2009. Constitutive ablation of dendritic cells breaks self-tolerance of CD4 T cells and results in spontaneous fatal autoimmunity. *J Exp Med* 206: 549-559.

17. Birnberg, T., L. Bar-On, A. Sapoznikov, M. L. Caton, L. Cervantes-Barragan, D. Makia, R. Krauthgamer, O. Brenner, B. Ludewig, D. Brockschnieder, D. Riethmacher, B. Reizis, and S. Jung. 2008. Lack of conventional dendritic cells is compatible with normal development and T cell homeostasis, but causes myeloid proliferative syndrome. *Immunity* 29: 986-997.
18. Esterhazy, D., J. Loschko, M. London, V. Jove, T. Y. Oliveira, and D. Mucida. 2016. Classical dendritic cells are required for dietary antigen-mediated induction of peripheral T(reg) cells and tolerance. *Nat Immunol* 17: 545-555.
19. Riemann, M., N. Andreas, M. Fedoseeva, E. Meier, D. Weih, H. Freytag, R. Schmidt-Ullrich, U. Klein, Z. Q. Wang, and F. Weih. 2017. Central immune tolerance depends on crosstalk between the classical and alternative NF-kappaB pathways in medullary thymic epithelial cells. *J Autoimmun* 81: 56-67.
20. Ishikawa, H., D. Carrasco, E. Claudio, R. P. Ryseck, and R. Bravo. 1997. Gastric hyperplasia and increased proliferative responses of lymphocytes in mice lacking the COOH-terminal ankyrin domain of NF-kappaB2. *The Journal of experimental medicine* 186: 999-1014.
21. Pichery, M., E. Mirey, P. Mercier, E. Lefrancais, A. Dujardin, N. Ortega, and J. P. Girard. 2012. Endogenous IL-33 is highly expressed in mouse epithelial barrier tissues, lymphoid organs, brain, embryos, and inflamed tissues: in situ analysis using a novel Il-33-LacZ gene trap reporter strain. *Journal of immunology* 188: 3488-3495.
22. Bettelli, E., Y. Carrier, W. Gao, T. Korn, T. B. Strom, M. Oukka, H. L. Weiner, and V. K. Kuchroo. 2006. Reciprocal developmental pathways for the generation of pathogenic effector TH17 and regulatory T cells. *Nature* 441: 235-238.
23. Bettelli, E., M. Pagany, H. L. Weiner, C. Linington, R. A. Sobel, and V. K. Kuchroo. 2003. Myelin oligodendrocyte glycoprotein-specific T cell receptor transgenic mice develop spontaneous autoimmune optic neuritis. *The Journal of experimental medicine* 197: 1073-1081.
24. Barnden, M. J., J. Allison, W. R. Heath, and F. R. Carbone. 1998. Defective TCR expression in transgenic mice constructed using cDNA-based alpha- and beta-chain genes under the control of heterologous regulatory elements. *Immunol Cell Biol* 76: 34-40.
25. Caton, M. L., M. R. Smith-Raska, and B. Reizis. 2007. Notch-RBP-J signaling controls the homeostasis of CD8- dendritic cells in the spleen. *J Exp Med* 204: 1653-1664.
26. De Silva, N. S., K. Silva, M. M. Anderson, G. Bhagat, and U. Klein. 2016. Impairment of Mature B Cell Maintenance upon Combined Deletion of the Alternative NF-kappaB Transcription Factors RELB and NF-kappaB2 in B Cells. *Journal of immunology* 196: 2591-2601.
27. Zhou, X., L. T. Jeker, B. T. Fife, S. Zhu, M. S. Anderson, M. T. McManus, and J. A. Bluestone. 2008. Selective miRNA disruption in T reg cells leads to uncontrolled autoimmunity. *The Journal of experimental medicine* 205: 1983-1991.
28. Soza-Ried, C., C. C. Bleul, M. Schorpp, and T. Boehm. 2008. Maintenance of thymic epithelial phenotype requires extrinsic signals in mouse and zebrafish. *Journal of immunology* 181: 5272-5277.
29. Wan, Y. Y., and R. A. Flavell. 2005. Identifying Foxp3-expressing suppressor T cells with a bicistronic reporter. *Proceedings of the National Academy of Sciences of the United States of America* 102: 5126-5131.
30. Brunkow, M. E., E. W. Jeffery, K. A. Hjerrild, B. Paeper, L. B. Clark, S. A. Yasayko, J. E. Wilkinson, D. Galas, S. F. Ziegler, and F. Ramsdell. 2001. Disruption of a new forkhead/winged-helix protein, scurfin, results in the fatal lymphoproliferative disorder of the scurfy mouse. *Nat Genet* 27: 68-73.
31. Wu, T. D., and S. Nacu. 2010. Fast and SNP-tolerant detection of complex variants and splicing in short reads. *Bioinformatics* 26: 873-881.
32. DeLuca, D. S., J. Z. Levin, A. Sivachenko, T. Fennell, M. D. Nazaire, C. Williams, M. Reich, W. Winckler, and G. Getz. 2012. RNA-SeQC: RNA-seq metrics for quality control and process optimization. *Bioinformatics* 28: 1530-1532.
33. Liao, Y., G. K. Smyth, and W. Shi. 2014. featureCounts: an efficient general purpose program for assigning sequence reads to genomic features. *Bioinformatics* 30: 923-930.
34. Love, M. I., W. Huber, and S. Anders. 2014. Moderated estimation of fold change and dispersion for RNA-seq data with DESeq2. *Genome Biol* 15: 550.

35. Weih, F., D. Carrasco, S. K. Durham, D. S. Barton, C. A. Rizzo, R. P. Ryseck, S. A. Lira, and R. Bravo. 1995. Multiorgan inflammation and hematopoietic abnormalities in mice with a targeted disruption of RelB, a member of the NF-kappa B/Rel family. *Cell* 80: 331-340.
36. Weih, F., S. K. Durham, D. S. Barton, W. C. Sha, D. Baltimore, and R. Bravo. 1996. Both multiorgan inflammation and myeloid hyperplasia in RelB-deficient mice are T cell dependent. *J Immunol* 157: 3974-3979.
37. Barton, D., H. HogenEsch, and F. Weih. 2000. Mice lacking the transcription factor RelB develop T cell-dependent skin lesions similar to human atopic dermatitis. *Eur J Immunol* 30: 2323-2332.
38. Grinberg-Bleyer, Y., R. Caron, J. J. Seeley, N. S. De Silva, C. W. Schindler, M. S. Hayden, U. Klein, and S. Ghosh. 2018. The Alternative NF-kappaB Pathway in Regulatory T Cell Homeostasis and Suppressive Function. *J Immunol* 200: 2362-2371.
39. Li, J., S. Chen, W. Chen, Q. Ye, Y. Dou, Y. Xiao, L. Zhang, L. J. Minze, X. C. Li, and X. Xiao. 2018. Role of the NF-kappaB Family Member RelB in Regulation of Foxp3(+) Regulatory T Cells In Vivo. *J Immunol* 200: 1325-1334.
40. Shih, V. F., J. Davis-Turak, M. Macal, J. Q. Huang, J. Ponomarenko, J. D. Kearns, T. Yu, R. Fagerlund, M. Asagiri, E. I. Zuniga, and A. Hoffmann. 2012. Control of RelB during dendritic cell activation integrates canonical and noncanonical NF-kappaB pathways. *Nat Immunol* 13: 1162-1170.
41. Wu, L., A. D'Amico, K. D. Winkel, M. Suter, D. Lo, and K. Shortman. 1998. RelB is essential for the development of myeloid-related CD8alpha- dendritic cells but not of lymphoid-related CD8alpha+ dendritic cells. *Immunity* 9: 839-847.
42. Briseno, C. G., M. Gargaro, V. Durai, J. T. Davidson, D. J. Theisen, D. A. Anderson, 3rd, D. V. Novack, T. L. Murphy, and K. M. Murphy. 2017. Deficiency of transcription factor RelB perturbs myeloid and DC development by hematopoietic-extrinsic mechanisms. *Proc Natl Acad Sci U S A* 114: 3957-3962.
43. Andreas, N., M. Riemann, C. N. Castro, M. Groth, I. Koliesnik, C. Engelmann, T. Sparwasser, T. Kamradt, R. Haenold, and F. Weih. 2018. A new RelB-dependent CD117(+) CD172a(+) murine dendritic cell subset preferentially induces Th2 differentiation and supports airway hyperresponses in vivo. *Eur J Immunol*.
44. Kretschmer, K., I. Apostolou, D. Hawiger, K. Khazaie, M. C. Nussenzweig, and H. von Boehmer. 2005. Inducing and expanding regulatory T cell populations by foreign antigen. *Nat Immunol* 6: 1219-1227.
45. Proietto, A. I., S. van Dommelen, P. Zhou, A. Rizzitelli, A. D'Amico, R. J. Steptoe, S. H. Naik, M. H. Lahoud, Y. Liu, P. Zheng, K. Shortman, and L. Wu. 2008. Dendritic cells in the thymus contribute to T-regulatory cell induction. *Proceedings of the National Academy of Sciences of the United States of America* 105: 19869-19874.
46. Li, J., J. Park, D. Foss, and I. Goldschneider. 2009. Thymus-homing peripheral dendritic cells constitute two of the three major subsets of dendritic cells in the steady-state thymus. *The Journal of experimental medicine* 206: 607-622.
47. Thiault, N., J. Darrigues, V. Adoue, M. Gros, B. Binet, C. Perals, B. Leobon, N. Fazilleau, O. P. Joffre, E. A. Robey, J. P. van Meerwijk, and P. Romagnoli. 2015. Peripheral regulatory T lymphocytes recirculating to the thymus suppress the development of their precursors. *Nat Immunol* 16: 628-634.
48. Kieback, E., E. Hilgenberg, U. Stervbo, V. Lampropoulou, P. Shen, M. Bunse, Y. Jaimes, P. Boudinot, A. Radbruch, U. Klemm, A. A. Kuhl, R. Liblau, N. Hoevelmeyer, S. M. Anderton, W. Uckert, and S. Fillatreau. 2016. Thymus-Derived Regulatory T Cells Are Positively Selected on Natural Self-Antigen through Cognate Interactions of High Functional Avidity. *Immunity* 44: 1114-1126.
49. Legoux, F. P., J. B. Lim, A. W. Cauley, S. Dikiy, J. Ertelt, T. J. Mariani, T. Sparwasser, S. S. Way, and J. J. Moon. 2015. CD4(+) T Cell Tolerance to Tissue-Restricted Self Antigens Is Mediated by Antigen-Specific Regulatory T Cells Rather Than Deletion. *Immunity* 43: 896-908.
50. Kitagawa, Y., N. Ohkura, Y. Kidani, A. Vandenbon, K. Hirota, R. Kawakami, K. Yasuda, D. Motooka, S. Nakamura, M. Kondo, I. Taniuchi, T. Kohwi-Shigematsu, and S. Sakaguchi. 2017. Guidance of regulatory T cell development by Satb1-dependent super-enhancer establishment. *Nat Immunol* 18: 173-183.

51. Schiering, C., T. Krausgruber, A. Chomka, A. Frohlich, K. Adelmann, E. A. Wohlfert, J. Pott, T. Griseri, J. Bollrath, A. N. Hegazy, O. J. Harrison, B. M. Owens, M. Lohning, Y. Belkaid, P. G. Fallon, and F. Powrie. 2014. The alarmin IL-33 promotes regulatory T-cell function in the intestine. *Nature* 513: 564-568.
52. Chen, C. C., T. Kobayashi, K. Iijima, F. C. Hsu, and H. Kita. 2017. IL-33 dysregulates regulatory T cells and impairs established immunologic tolerance in the lungs. *J Allergy Clin Immunol* 140: 1351-1363 e1357.
53. Liew, F. Y., J. P. Girard, and H. R. Turnquist. 2016. Interleukin-33 in health and disease. *Nat Rev Immunol* 16: 676-689.
54. Siede, J., A. Frohlich, A. Datsi, A. N. Hegazy, D. V. Varga, V. Holecska, H. Saito, S. Nakae, and M. Lohning. 2016. IL-33 Receptor-Expressing Regulatory T Cells Are Highly Activated, Th2 Biased and Suppress CD4 T Cell Proliferation through IL-10 and TGFbeta Release. *PloS one* 11: e0161507.
55. Noval Rivas, M., O. T. Burton, P. Wise, L. M. Charbonnier, P. Georgiev, H. C. Oettgen, R. Rachid, and T. A. Chatila. 2015. Regulatory T cell reprogramming toward a Th2-cell-like lineage impairs oral tolerance and promotes food allergy. *Immunity* 42: 512-523.
56. Kim, K. S., S. W. Hong, D. Han, J. Yi, J. Jung, B. G. Yang, J. Y. Lee, M. Lee, and C. D. Surh. 2016. Dietary antigens limit mucosal immunity by inducing regulatory T cells in the small intestine. *Science*.
57. Korn, T., M. Mitsdoerffer, A. L. Croxford, A. Awasthi, V. A. Dardalhon, G. Galileos, P. Vollmar, G. L. Stritesky, M. H. Kaplan, A. Waisman, V. K. Kuchroo, and M. Oukka. 2008. IL-6 controls Th17 immunity in vivo by inhibiting the conversion of conventional T cells into Foxp3+ regulatory T cells. *Proc Natl Acad Sci U S A* 105: 18460-18465.
58. Jiang, H. R., M. Milovanovic, D. Allan, W. Niedbala, A. G. Besnard, S. Y. Fukada, J. C. Alves-Filho, D. Togbe, C. S. Goodyear, C. Linington, D. Xu, M. L. Lukic, and F. Y. Liew. 2012. IL-33 attenuates EAE by suppressing IL-17 and IFN-gamma production and inducing alternatively activated macrophages. *Eur J Immunol* 42: 1804-1814.
59. Hawiger, D., K. Inaba, Y. Dorsett, M. Guo, K. Mahnke, M. Rivera, J. V. Ravetch, R. M. Steinman, and M. C. Nussenzweig. 2001. Dendritic cells induce peripheral T cell unresponsiveness under steady state conditions in vivo. *The Journal of experimental medicine* 194: 769-779.
60. Darrasse-Jeze, G., S. Deroubaix, H. Mouquet, G. D. Victora, T. Eisenreich, K. H. Yao, R. F. Masilamani, M. L. Dustin, A. Rudensky, K. Liu, and M. C. Nussenzweig. 2009. Feedback control of regulatory T cell homeostasis by dendritic cells in vivo. *The Journal of experimental medicine* 206: 1853-1862.
61. Vahl, J. C., C. Drees, K. Heger, S. Heink, J. C. Fischer, J. Nedjic, N. Ohkura, H. Morikawa, H. Poeck, S. Schallenberg, D. Riess, M. Y. Hein, T. Buch, B. Polic, A. Schonle, R. Zeiser, A. Schmitt-Graff, K. Kretschmer, L. Klein, T. Korn, S. Sakaguchi, and M. Schmidt-Supprian. 2014. Continuous T cell receptor signals maintain a functional regulatory T cell pool. *Immunity* 41: 722-736.
62. Levine, A. G., A. Arvey, W. Jin, and A. Y. Rudensky. 2014. Continuous requirement for the TCR in regulatory T cell function. *Nat Immunol* 15: 1070-1078.
63. Matta, B. M., J. M. Lott, L. R. Mathews, Q. Liu, B. R. Rosborough, B. R. Blazar, and H. R. Turnquist. 2014. IL-33 is an unconventional Alarmin that stimulates IL-2 secretion by dendritic cells to selectively expand IL-33R/ST2+ regulatory T cells. *Journal of immunology* 193: 4010-4020.
64. Williams, J. W., M. Y. Tjota, B. S. Clay, B. Vander Lugt, H. S. Bandukwala, C. L. Hrusch, D. C. Decker, K. M. Blaine, B. R. Fixsen, H. Singh, R. Sciammas, and A. I. Sperling. 2013. Transcription factor IRF4 drives dendritic cells to promote Th2 differentiation. *Nat Commun* 4: 2990.
65. Dohler, A., T. Schneider, I. Eckert, E. Ribechini, N. Andreas, M. Riemann, B. Reizis, F. Weih, and M. B. Lutz. 2017. RelB(+) Steady-State Migratory Dendritic Cells Control the Peripheral Pool of the Natural Foxp3(+) Regulatory T Cells. *Front Immunol* 8: 726.
66. Yang, B. H., S. Hagemann, P. Mamareli, U. Lauer, U. Hoffmann, M. Beckstette, L. Fohse, I. Prinz, J. Pezoldt, S. Suerbaum, T. Sparwasser, A. Hamann, S. Floess, J. Huehn, and M. Lochner. 2015. Foxp3 T cells expressing RORgammat represent a stable regulatory T-cell effector lineage with enhanced suppressive capacity during intestinal inflammation. *Mucosal Immunol*.

67. Xu, M., M. Pokrovskii, Y. Ding, R. Yi, C. Au, O. J. Harrison, C. Galan, Y. Belkaid, R. Bonneau, and D. R. Littman. 2018. c-MAF-dependent regulatory T cells mediate immunological tolerance to a gut pathobiont. *Nature* 554: 373-377.
68. Han, D., M. C. Walsh, P. J. Cejas, N. N. Dang, Y. F. Kim, J. Kim, L. Charrier-Hisamuddin, L. Chau, Q. Zhang, K. Bittinger, F. D. Bushman, L. A. Turka, H. Shen, B. Reizis, A. L. Defranco, G. D. Wu, and Y. Choi. 2013. Dendritic cell expression of the signaling molecule TRAF6 is critical for gut microbiota-dependent immune tolerance. *Immunity* 38: 1211-1222.
69. Ovadia, A., Y. Dinur Schejter, E. Grunebaum, V. H. Kim, B. Reid, T. Schechter, E. Pope, and C. M. Roifman. 2017. Hematopoietic stem cell transplantation for RelB deficiency. *J Allergy Clin Immunol* 140: 1199-1201 e1193.
70. Li, M., X. Zhang, X. Zheng, D. Lian, Z. X. Zhang, W. Ge, J. Yang, C. Vladau, M. Suzuki, D. Chen, R. Zhong, B. Garcia, A. M. Jevnikar, and W. P. Min. 2007. Immune modulation and tolerance induction by RelB-silenced dendritic cells through RNA interference. *Journal of immunology* 178: 5480-5487.
71. Yang, H., Y. Zhang, M. Wu, J. Li, W. Zhou, G. Li, X. Li, B. Xiao, and P. Christadoss. 2010. Suppression of ongoing experimental autoimmune myasthenia gravis by transfer of RelB-silenced bone marrow dentritic cells is associated with a change from a T helper Th17/Th1 to a Th2 and FoxP3+ regulatory T-cell profile. *Inflamm Res* 59: 197-205.
72. Zhu, H. C., T. Qiu, X. H. Liu, W. C. Dong, X. D. Weng, C. H. Hu, Y. L. Kuang, R. H. Gao, C. Dan, and T. Tao. 2012. Tolerogenic dendritic cells generated by RelB silencing using shRNA prevent acute rejection. *Cell Immunol* 274: 12-18.
73. Nair, P. M., M. R. Starkey, T. J. Haw, R. Ruscher, G. Liu, M. R. Maradana, R. Thomas, B. J. O'Sullivan, and P. M. Hansbro. 2018. RelB-Deficient Dendritic Cells Promote the Development of Spontaneous Allergic Airway Inflammation. *Am J Respir Cell Mol Biol* 58: 352-365.
74. Halim, L., M. Romano, R. McGregor, I. Correa, P. Pavlidis, N. Grageda, S. J. Hoong, M. Yuksel, W. Jassem, R. F. Hannen, M. Ong, O. McKinney, B. Hayee, S. N. Karagiannis, N. Powell, R. I. Lechler, E. Nova-Lamperti, and G. Lombardi. 2017. An Atlas of Human Regulatory T Helper-like Cells Reveals Features of Th2-like Tregs that Support a Tumorigenic Environment. *Cell Rep* 20: 757-770.

Footnotes

T.K. is supported by the DFG (SFB1054-B6 and TR128-A7), by the BMBF (T-B in NMO), and by the European Research Council (ERC-CoG EXODUS). F.W. has been supported by the Deutsche Forschungsgemeinschaft (WE 2224/6 and WE 2224/6-2). C.O. is supported by the European Research Council (ERC) of the European Union's Horizon 2020 framework program (ERC-StG 716718) and by the Deutsche Forschungsgemeinschaft (within FOR2559 - OH 282/1-1).

Figure legends

Figure 1. Differential impact of alternative NF-κB member on DCs and Tregs

A) Frequencies of Foxp3^{+} Tregs among CD4^{+} T cells in spleens of the indicated knockout animals or bone-marrow chimeras.

B) Frequencies of Foxp3^{+} Tregs among CD4^{+} T cells in spleens of the indicated conditional knockout animals.

C) Bar diagrams show frequencies of splenic DCs and Sirpα^{+}CD8α^{-} and Sirpα^{-}CD8α^{+} DC subsets (upper panels) of control and RelB$^{\Delta DC}$ mice. Contour plots (lower panels) show DEC-205^{+}Sirpα^{-} splenic DC subsets and enumeration in control and RelB$^{\Delta DC}$ mice.

D) Bar diagrams show frequencies of splenic DCs and Sirpα^{+}CD8α^{-} and Sirpα^{-}CD8α^{+} DC subsets (upper panels) of control and NF-κB2$^{\Delta DC}$ mice. Contour plots (lower panels) show DEC-205^{+}Sirpα^{-} splenic DC subsets and enumeration in control and NF-κB2$^{\Delta DC}$ mice.

E) Representative histograms and mean fluorescence intensity (MFI) of PD-L1, PD-L2 and OX40L expression on dendritic cells (CD11c^{+}MHC-II^{+}) in spleens from littermate control (filled histogram) or RelB$^{\Delta DC}$ mice (open histograms).

F) Quantification of Treg frequencies in the thymi of 1-week and 2-week-old littermate controls and RelB$^{\Delta DC}$ mice.

G) Quantification of Foxp3^{+} Treg frequencies in spleen and thymus of wildtype or RelB$^{\Delta DC}$ mice or mice lacking RelB in medullary thymic epithelial cells (RelB$^{\Delta TEC}$) or both (RelB$^{\Delta DC\Delta TEC}$). Statistics were performed with One-Way-ANOVA with Turkey's multiple correction test (***P<0.001).

All data show pooled results of at least two independent experiments and if not stated differently, analyzed by two-tailed student's t test. Bar diagrams show mean± SD. *P<0.05, **P<0.01, ***P<0.001

Figure 2: Accumulated Tregs in RelB$^{\Delta DC}$ mice show a tissue Treg signature with a type 2 immune bias

A) Representative FACS plots and quantification of Foxp3^{+} Tregs among CD4^{+} T cells and frequency of Helios^{+} among total Tregs in indicated organs. Statistics were performed with One-Way-ANOVA with Turkey's multiple correction test.

B) Bar diagrams show frequencies of Ki-67^{+} cells among Foxp3^{+} Tregs in indicated organs.

C) Heatmap depicts selected differentially expressed genes according to RNA-seq analysis of sort-purified Tregs isolated from the peritoneal cavity (PEC) of control or RelB$^{\Delta DC}$ mice with an FDR < 0.1 and adjusted P<0.1.

D) Quantification of selected tissue Treg marker expression in PEC by flow cytometry.

E) Representative FACS plots and quantification of Gata3^{hi}Helios^{+} and Gata3^{hi}Helios^{-} within pregated Foxp3^{+} Tregs isolated from the lamina propria of the small intestine.

F) Representative FACS plots (left) and bar diagrams (right) of RORγt and Gata3 expression within pregated Foxp3^{+} Tregs isolated from the lamina propria of the small intestine and ratio between Gata3 and RORγt expressing Tregs.

G) Bar diagrams show frequencies of RORγt^{+} and Gata3^{hi} T cells among Foxp3^{-} T effector cells ratio between Gata3 and RORγt expressing T effector cells isolated from the small intestine.

H) Concentration of total serum IgE level of naïve adult mice.

All data show pooled results of at least two independent experiments and analyzed if not stated differently, by two-tailed student's t test. Bar diagrams show mean± SD. *P<0.05, **P<0.01, ***P<0.001.

Figure 3: RelB$^{\Delta DC}$ mice accumulate ST2^{+} tissue Tregs independent of IL-33

A) Representative FACS plots (left) and quantification (right) of Gata3^{+}ST2^{+} cells within Foxp3^{-} T cells in PEC or small intestine of littermate control and RelB$^{\Delta DC}$ mice.

B) Representative FACS plots (left) and quantification (right) from littermate control and RelB$^{\Delta DC}$ mice showing ST2^{+} Helios^{+} cells among Foxp3^{+} Tregs from PEC and lamina propria of the small intestine.

C) IL-33 and IL-2 serum levels of control littermates and RelB$^{\Delta DC}$ mice.

D) sST2 or PBS was injected i.p every other day into control or RelB$^{\Delta DC}$ mice for three weeks. Bars indicate Foxp3^{+} Treg numbers and ST2 expression among Tregs in the spleen at the end of the experiment. Statistics were performed with One-Way-ANOVA with Turkey's multiple correction test. *P<0.05, **P<0.01, ***P<0.001, ****P<0.0001.

E) Treg frequencies and expression of Helios, ST2 and Gata3 in the spleen from bone marrow chimeras receiving either bone marrow from littermate or RelB$^{\Delta DC}$ animals. Wildype or IL-33$^{KO/KO}$ animals served as recipients as indicated. Lower plots show serum levels of IL-33 or IL-2 in the described bone marrow chimeras. Statistics were performed with One-Way-ANOVA with Turkey's multiple correction test. *P<0.05, **P<0.01, ***P<0.001, ****P<0.0001.

All data show pooled results of one (E) or at least two independent experiments and analyzed if not stated differently, by two-tailed student's t test. Bar diagrams show mean± SD. *P<0.05, **P<0.01, ***P<0.001.

Figure 4: Tregs from RelB$^{\Delta DC}$ mice are functional *in vitro* and *in vivo* but *de novo* induction of Tregs in the intestinal tract is impaired.

A) Proliferation index from an *in vitro* suppression assay with DCs and effector T cells isolated from wildtype mice and Tregs isolated from littermate control or RelB$^{\Delta DC}$ mice.

B) 6-day old mice with the scurfy mutation received bulk CD4^{+} T cells isolated from littermate control or RelB$^{\Delta DC}$ mice by intraperitoneal injection. Upper plot indicate survival rate, lower plot indicate mean percentage of initial body weight at day 20.

C) Littermate control and RelB$^{\Delta DC}$ mice were sensitized with BSA in CFA and challenged at day 6. Left plot shows mean footpad swelling after antigen challenge and right plot indicates frequency of cytokine positive cells among CD40L^{+} T helper cells after restimulation of popliteal lymph node cells.

D) Littermate control and RelB$^{\Delta DC}$ mice received congenically labeled naïve OT-II T cells by intravenous injection and were exposed to 1.5% chicken ovalbumin containing drinking water for the following nine days. Representative contour plots (above) and quantification (lower) of Foxp3^{+} and ROR(γt)$^{+}$Foxp3^{+} among OT-II cells isolated from the lamina propria of the small intestine are shown.

E) Comparison of endogenous and transferred T cells for Foxp3 and Gata3 expression among T effector cells isolated from the lamina propria of the small intestine from the experiment in D).

F) Quantification of the data shown in E).

All data show pooled results of at least two independent experiments and analyzed by two-tailed student's t test. Bar diagrams show mean± SD. *P<0.05, **P<0.01, ***P<0.001

Figure 5: RelB$^{\Delta DC}$ mice are protected from EAE due to accumulation of Tregs

EAE was induced by immunizing littermate control or RelB$^{\Delta DC}$ mice with MOG_{35-55} in CFA as described in material and methods.

A) EAE clinical score in WT and RelB$^{\Delta DC}$ mice shown as mean ± SEM of one representative experiment. Table depicts summary of all experiments. Sick = score of at least one. Mice that had to be sacrificed due to high disease scores are indicated as deaths.

B) Total numbers of cytokine-expressing T helper cells in the CNS at peak of disease after PMA/Iono restimulation of one representative experiment.

C) Frequency of Foxp3$^-$Gata3$^+$ and Foxp3$^+$Gata3$^+$ T helper cells in the CNS at peak of disease.

D) Frequency of Foxp3$^+$ cells within CD4$^+$ T cells or frequency of Helios$^+$ ST2$^+$ cells within Foxp3$^+$ Tregs in the CNS at peak of disease.

E) Clinical score of EAE in littermate control and RelB$^{\Delta DC}$ mice treated with an anti-CD25 antibody (open symbols) or PBS (filled symbols) prior induction of EAE as described in methods section. Diagram shows mean ± SEM.

F) Total cell number of cytokine-expressing Foxp3$^-$ CD4$^+$ T cells in the CNS at the peak of EAE.

G) Littermate control and RelB$^{\Delta DC}$ mice received 2.5x10^6 sort-purified MOG-specific Foxp3/GFP$^-$2D2 T cells prior EAE induction via intravenous injection. Upper plots (left) and quantification (right) indicate frequency of Vα3.2$^+$Vβ11$^+$ 2D2 cells among CD4$^+$ T cells isolated from draining inguinal lymph nodes at day 8 after EAE induction. Lower plots indicate frequency (left) and quantification (right) of Foxp3/GFP$^+$ cells among Vα3.2$^+$Vβ11$^+$ 2D2 T cells isolated from draining inguinal lymph nodes at day 8 after EAE induction.

Bar diagrams show mean ± SD of at least two independent experiments unless otherwise indicated. Statistical analysis was performed using Mann-Whitney-U test (in A)) or two-way ANOVA with Turkey's multiple correction test (in E). Otherwise, unpaired two-tailed Student's t test was used. *p<0,05, **p<0,01, ***p<0,001.

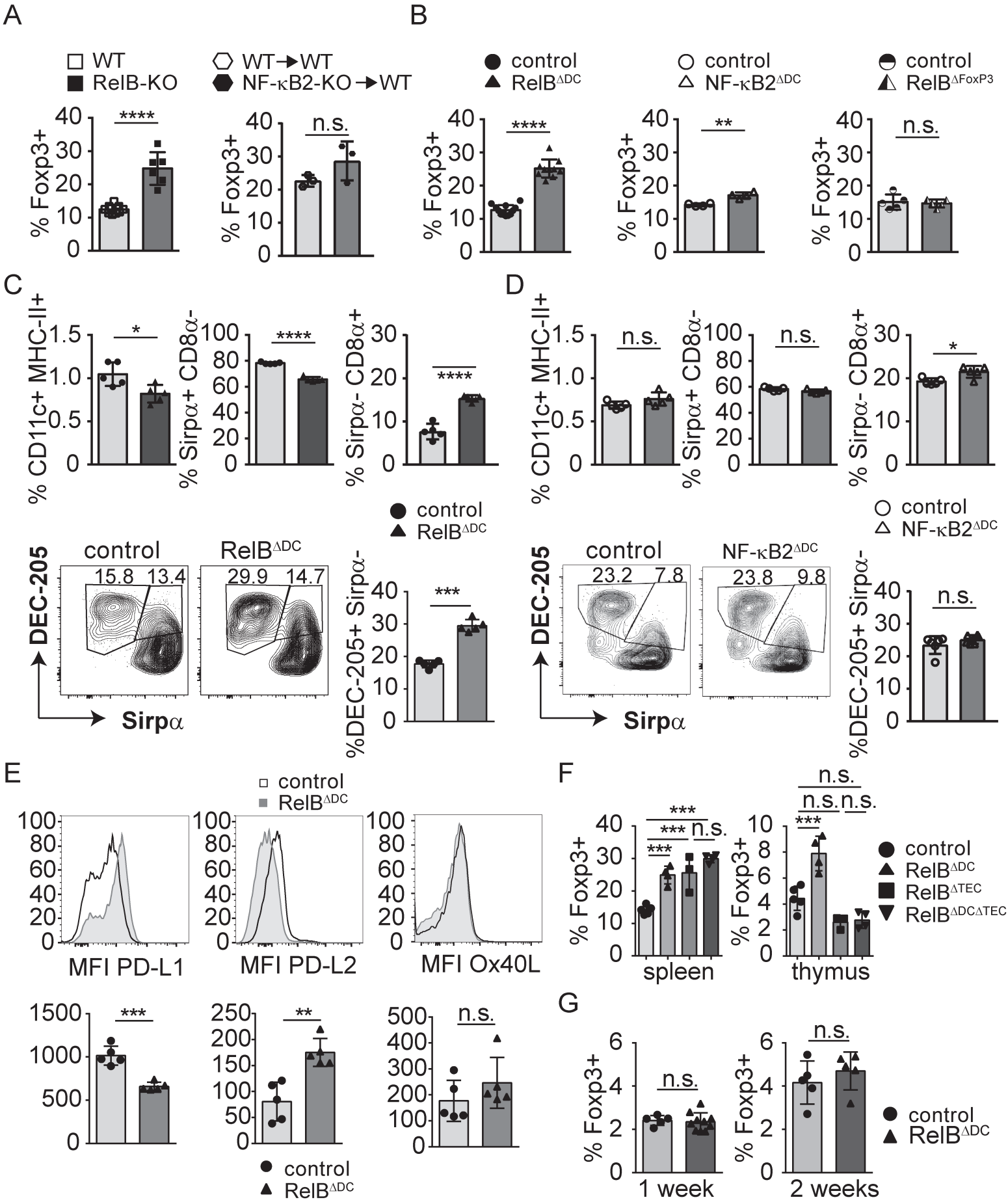
A
WT
RelB-KO
WT→WT
NF-κB2-KO→WT
% Foxp3+
****
n.s.
B
control
RelB^ΔDC
control
NF-κB2^ΔDC
control
RelB^ΔFoxP3
**
C
% CD11c+ MHC-II+
% Sirpα+ CD8α-
% Sirpα- CD8α+
*
****
control
RelB^ΔDC
control
RelB^ΔDC
DEC-205
Sirpα
15.8 13.4
29.9 14.7
%DEC-205+ Sirpα-
***
D
n.s.
*
control
NF-κB2^ΔDC
control
NF-κB2^ΔDC
23.2 7.8
23.8 9.8
E
control
RelB^ΔDC
MFI PD-L1
MFI PD-L2
MFI Ox40L
**
F
spleen
thymus
control
RelB^ΔDC
RelB^ΔTEC
RelB^ΔDCΔTEC
G
1 week
2 weeks
control
RelB^ΔDC

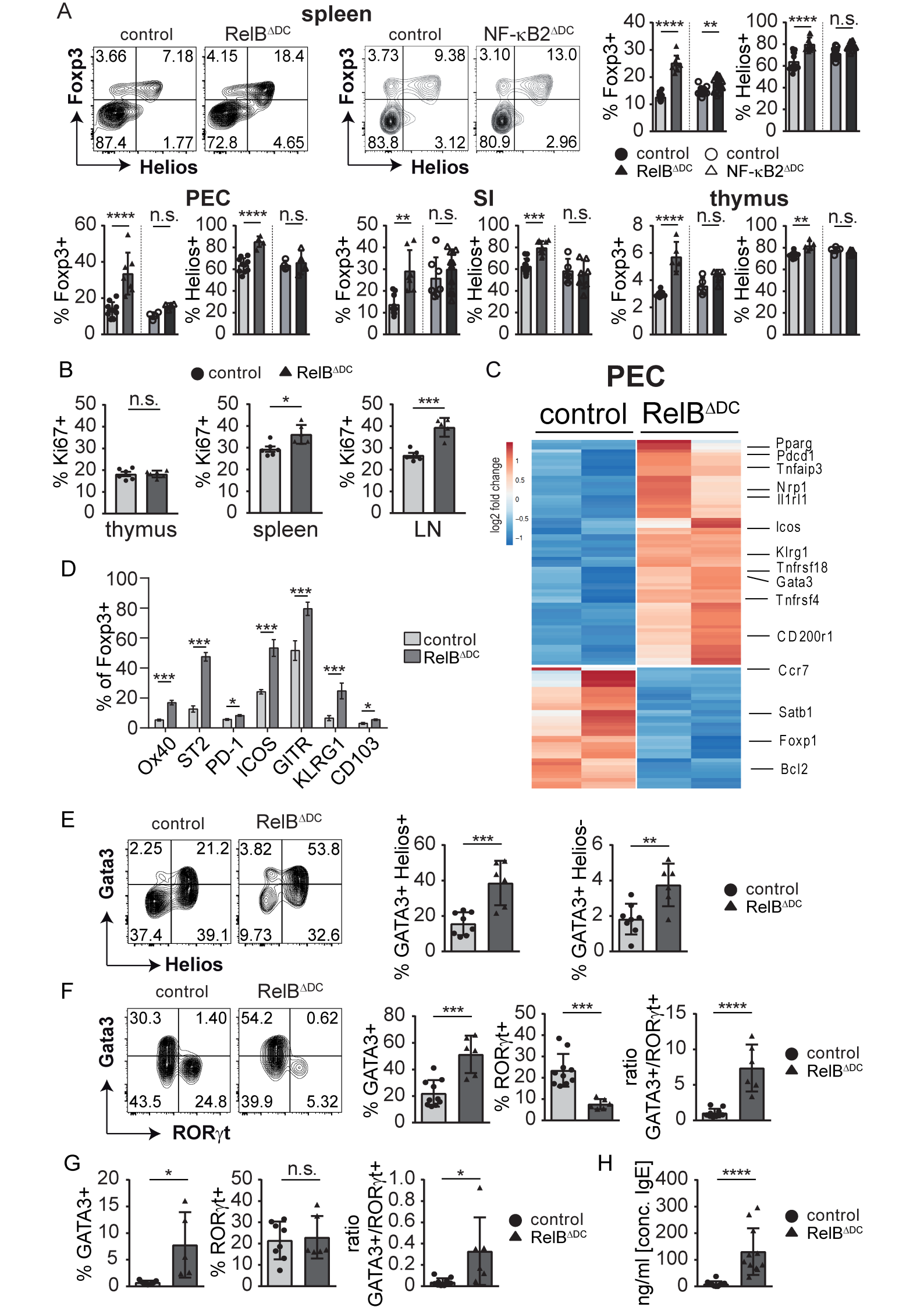
A
spleen
control
RelB$^{\Delta DC}$
NF-κB2$^{\Delta DC}$
Foxp3
Helios
3.66
7.18
87.4
1.77
4.15
18.4
72.8
4.65
3.73
9.38
83.8
3.12
3.10
13.0
80.9
2.96
% Foxp3+
% Helios+
PEC
SI
thymus
n.s.
B
% Ki67+
thymus
spleen
LN
C
PEC
log2 fold change
Pparg
Pdcd1
Tnfaip3
Nrp1
Il1rl1
Icos
Klrg1
Tnfrsf18
Gata3
Tnfrsf4
CD200r1
Ccr7
Satb1
Foxp1
Bcl2
D
% of Foxp3+
Ox40
ST2
PD-1
ICOS
GITR
KLRG1
CD103
E
Gata3
% GATA3+ Helios+
% GATA3+ Helios-
F
RORγt
% GATA3+
% RORγt+
ratio GATA3+/RORγt+
G
H
ng/ml [conc. IgE]

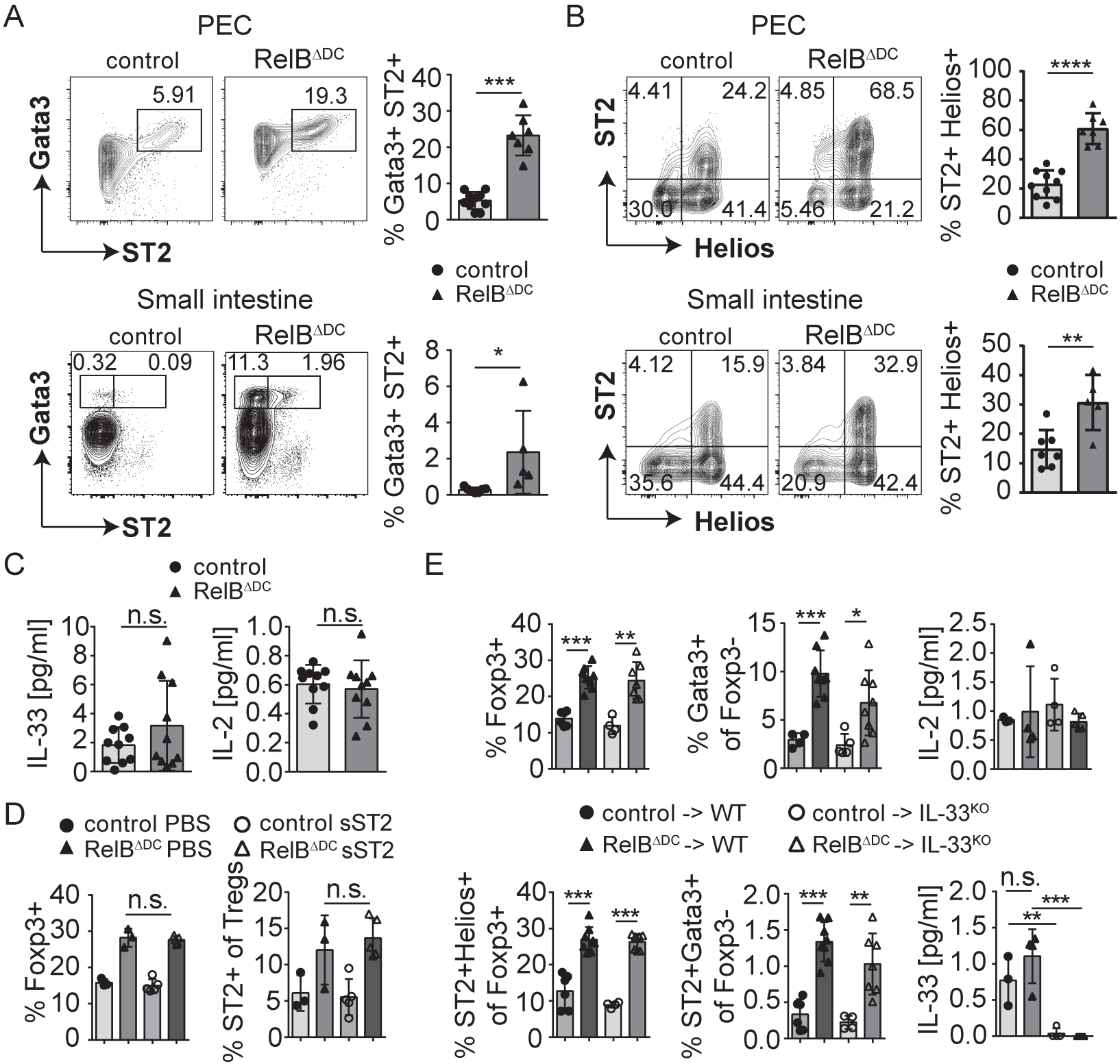
A
PEC
control
RelB^ΔDC
5.91
19.3
Gata3
ST2
% Gata3+ ST2+
***
control
RelB^ΔDC
Small intestine
0.32
0.09
11.3
1.96
*
B
4.41
24.2
30.0
41.4
4.85
68.5
5.46
21.2
Helios
% ST2+ Helios+
****
4.12
15.9
35.6
44.4
3.84
32.9
20.9
42.4
**
C
IL-33 [pg/ml]
IL-2 [pg/ml]
n.s.
D
control PBS
RelB^ΔDC PBS
control sST2
RelB^ΔDC sST2
% Foxp3+
% ST2+ of Tregs
E
% Foxp3+
% Gata3+ of Foxp3-
IL-2 [pg/ml]
control -> WT
RelB^ΔDC -> WT
control -> IL-33^KO
RelB^ΔDC -> IL-33^KO
% ST2+Helios+ of Foxp3+
% ST2+Gata3+ of Foxp3-
IL-33 [pg/ml]

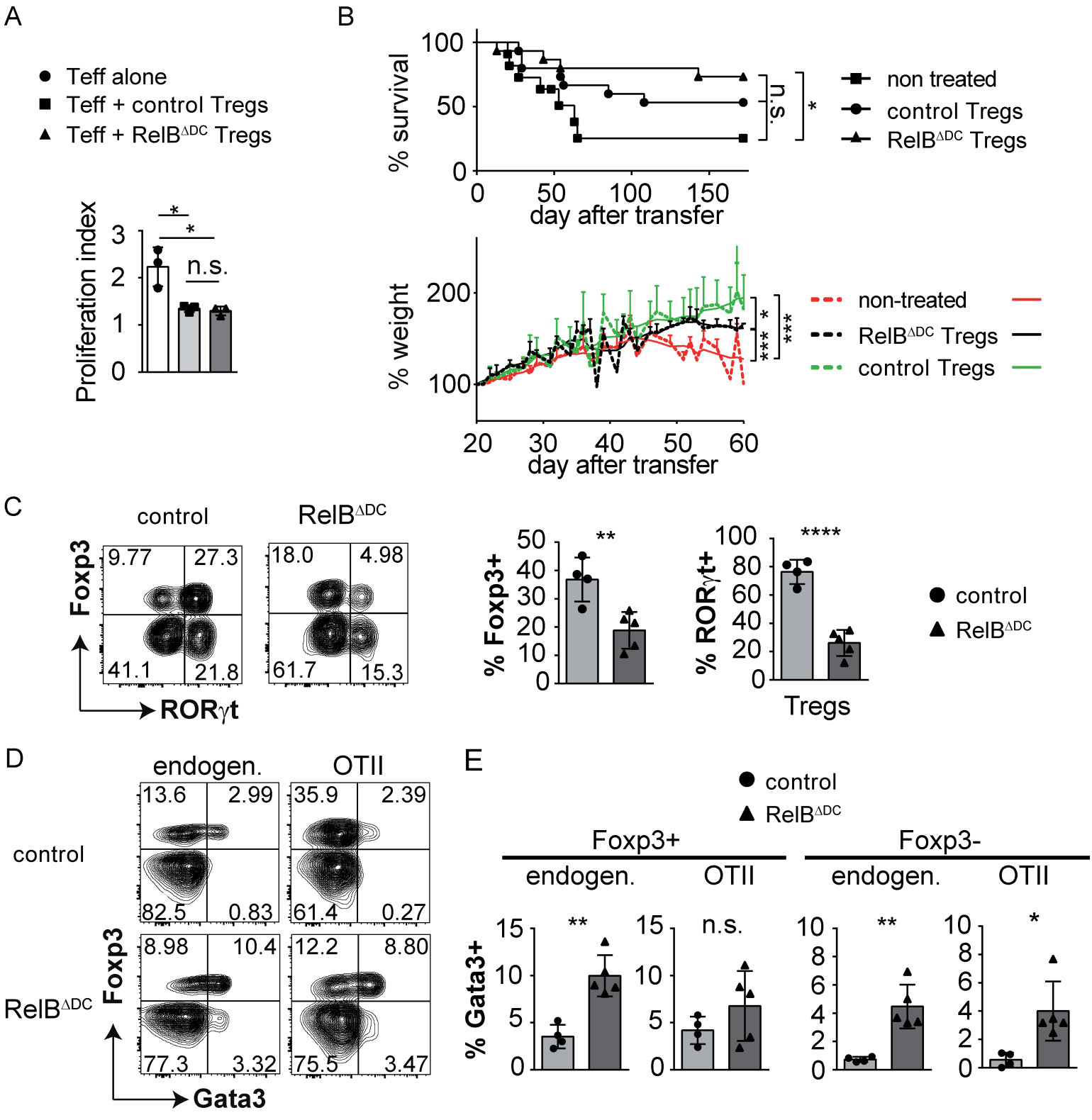
A
Teff alone
Teff + control Tregs
Teff + RelB^ΔDC Tregs
Proliferation index
n.s.
B
% survival
day after transfer
non treated
control Tregs
RelB^ΔDC Tregs
% weight
non-treated
RelB^ΔDC Tregs
control Tregs
C
control
RelB^ΔDC
Foxp3
RORγt
9.77
27.3
41.1
21.8
18.0
4.98
61.7
15.3
% Foxp3+
% RORγt+
Tregs
control
RelB^ΔDC
D
endogen.
OTII
control
RelB^ΔDC
Foxp3
Gata3
13.6
2.99
82.5
0.83
35.9
2.39
61.4
0.27
8.98
10.4
77.3
3.32
12.2
8.80
75.5
3.47
E
control
RelB^ΔDC
Foxp3+
Foxp3-
endogen.
OTII
% Gata3+
n.s.

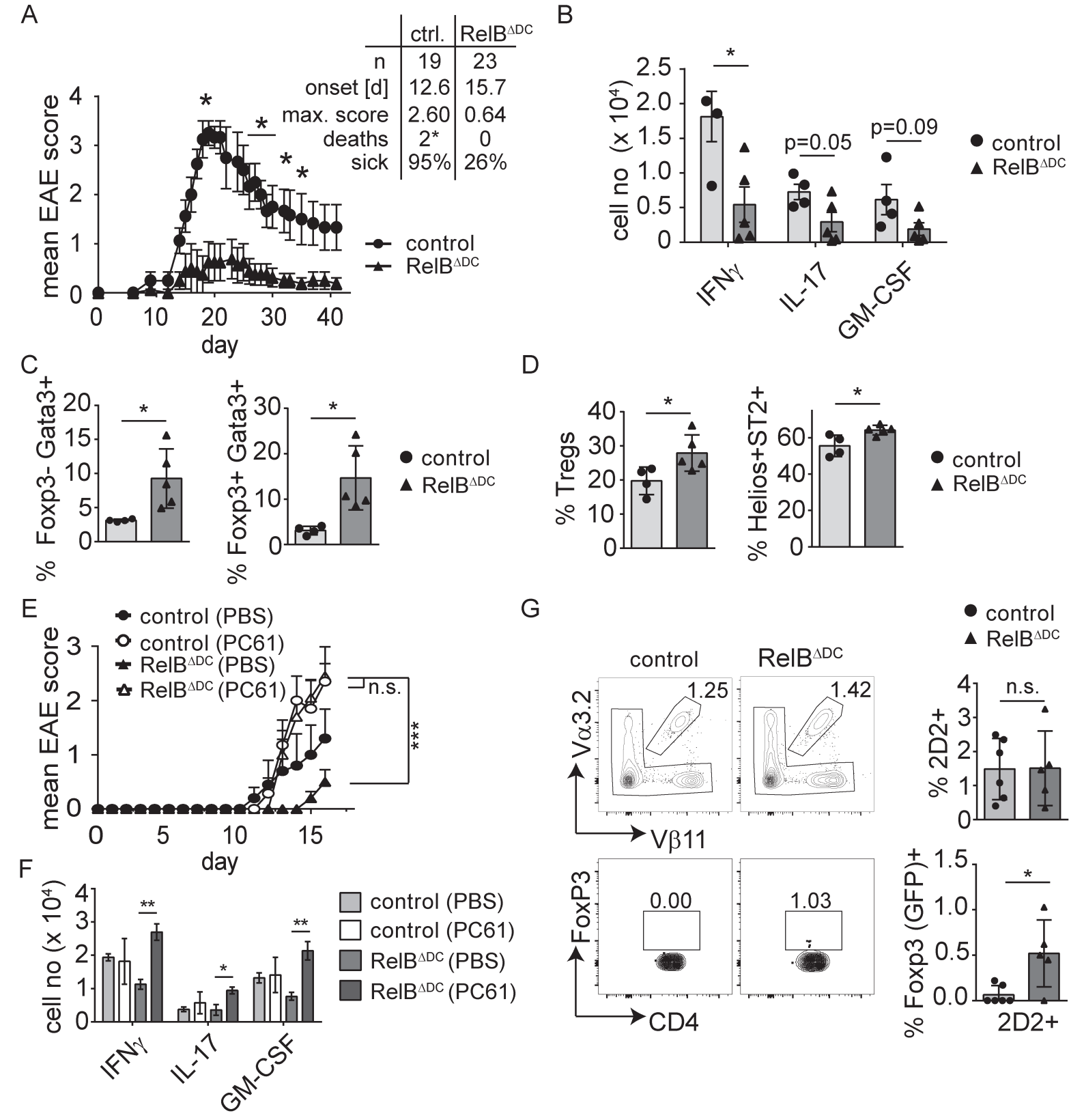
A
ctrl.
RelB^ΔDC
n 19 23
onset [d] 12.6 15.7
max. score 2.60 0.64
deaths 2* 0
sick 95% 26%
mean EAE score
day
control
RelB^ΔDC
B
cell no (x 10^4)
p=0.05
p=0.09
IFNγ
IL-17
GM-CSF
control
RelB^ΔDC
C
% Foxp3- Gata3+
% Foxp3+ Gata3+
control
RelB^ΔDC
D
% Tregs
% Helios+ST2+
control
RelB^ΔDC
E
control (PBS)
control (PC61)
RelB^ΔDC (PBS)
RelB^ΔDC (PC61)
n.s.
***
mean EAE score
day
F
cell no (x 10^4)
control (PBS)
control (PC61)
RelB^ΔDC (PBS)
RelB^ΔDC (PC61)
IFNγ
IL-17
GM-CSF
G
control
RelB^ΔDC
1.25
1.42
Vα3.2
Vβ11
0.00
1.03
FoxP3
CD4
control
RelB^ΔDC
n.s.
% 2D2+
% Foxp3 (GFP)+
2D2+

Suppl Fig 1

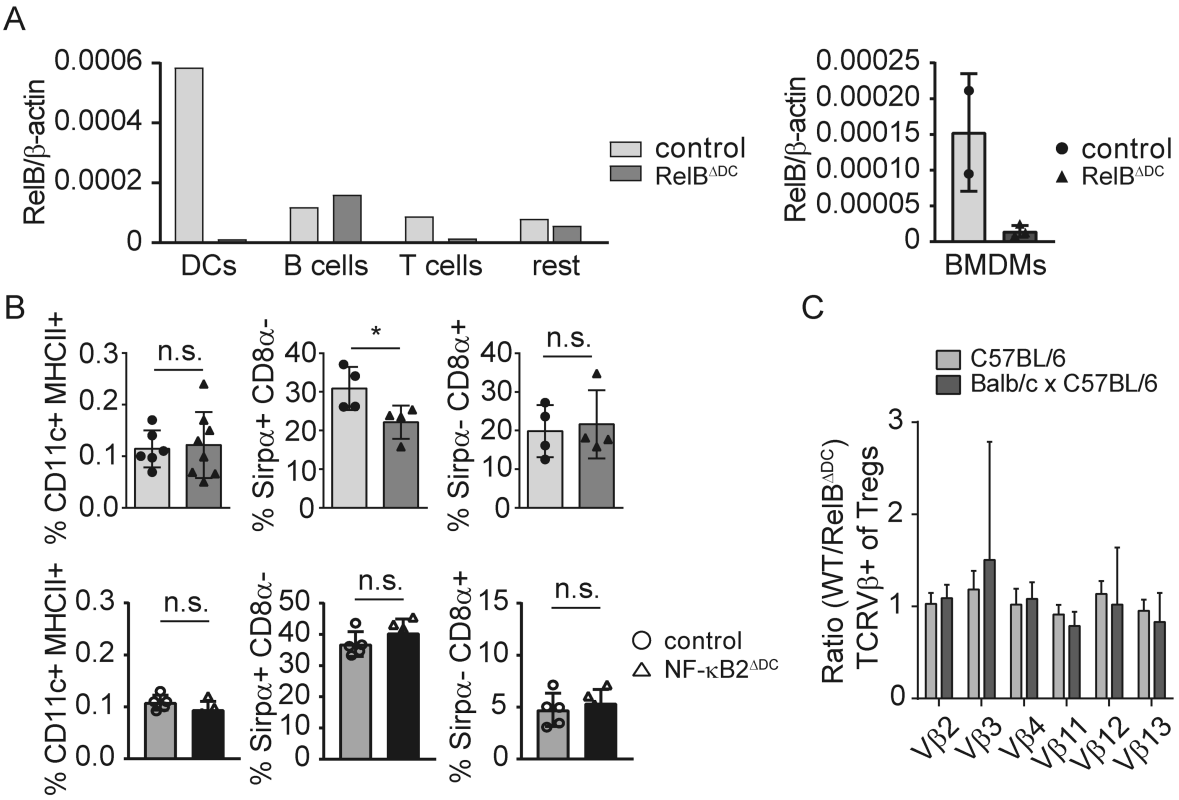

Supplementary Figure 1:

A) Left: relative expression of RelB to β-actin in DCs ($CD11c^{hi}MHC\text{-}II^{hi}$), T cells ($CD3^{+}$), B cells ($CD19^{+}$) and all other cells sort-purified from spleen. Right: relative expression of RelB to β-actin mRNA in GM-CSF differentiated BMDMs from littermate controls or $RelB^{\Delta DC}$ mice.

B) Frequency of $CD11c^{+}MHC\text{-}II^{+}$ DCs within living thymocytes and frequency of $Sirp\alpha^{+}CD8\alpha^{-}$ or $Sirp\alpha^{-}CD8\alpha^{+}$ cells among thymic DCs from $RelB^{\Delta DC}$ mice, NF-κ$B2^{\Delta DC}$ mice and their control littermates.

C) WT/$RelB^{\Delta DC}$ ratio of annotated TCRVβ chain frequency within thymic Tregs from mice with C57BL/6 or Balb/c x C57BL/6 mixed background.

All data were analyzed by two-tailed student's t test. Bar diagrams show mean ± SD. *P<0.05, **P<0.01, ***P<0.001.

Suppl Fig 2

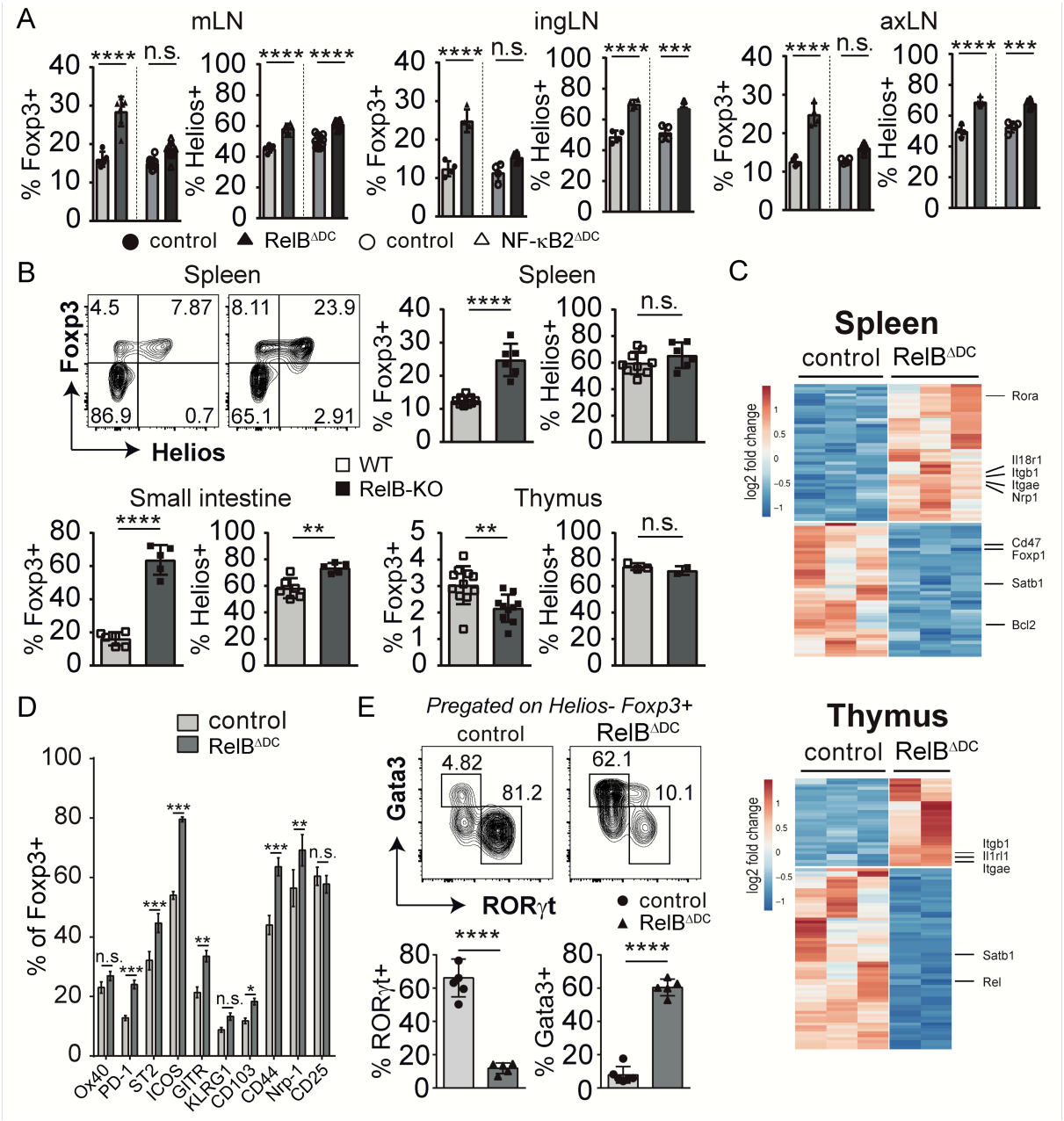

Supplementary Figure 2:

A) Frequencies of Foxp3$^+$ Tregs among CD4$^+$ T cells and frequency of Helios$^+$ among total Tregs in indicated organs. Statistics were performed with One-Way-ANOVA with Turkey's multiple correction test.

B) Representative FACS plots and quantification of Foxp3$^+$ Tregs within CD4$^+$ T cells and frequency of Helios$^+$ among total Tregs in indicated organs from RelB-KO mice or wildtype controls. For comparison reasons, the graph for the frequency of Tregs in the spleen shown in Figure 1A is depicted here again.

C) Heatmap depicts selected differentially expressed genes according to RNA_seq analysis of sort-purified Tregs isolated from the spleen and thymus of littermate controls or RelB$^{\Delta DC}$ mice with an FDR < 0.1 and adjusted P<0.1.

D) Quantification of indicated marker frequency among Tregs from the spleen of littermate

control or RelB$^{\Delta DC}$ mice.

E) Representative FACS plots (upper panel) and quantification (lower panel) among pregated Helios^{-}Foxp3^{+} T cells expressing Gata3 and RORγt isolated from the small intestine of littermate control and RelB$^{\Delta DC}$ mice.

All data show pooled results of at least two independent experiments and were analyzed by two tailed student's t test. Bar diagrams show mean ± SD. *P<0.05, **P<0.01, ***P<0.001.

Suppl Fig 3

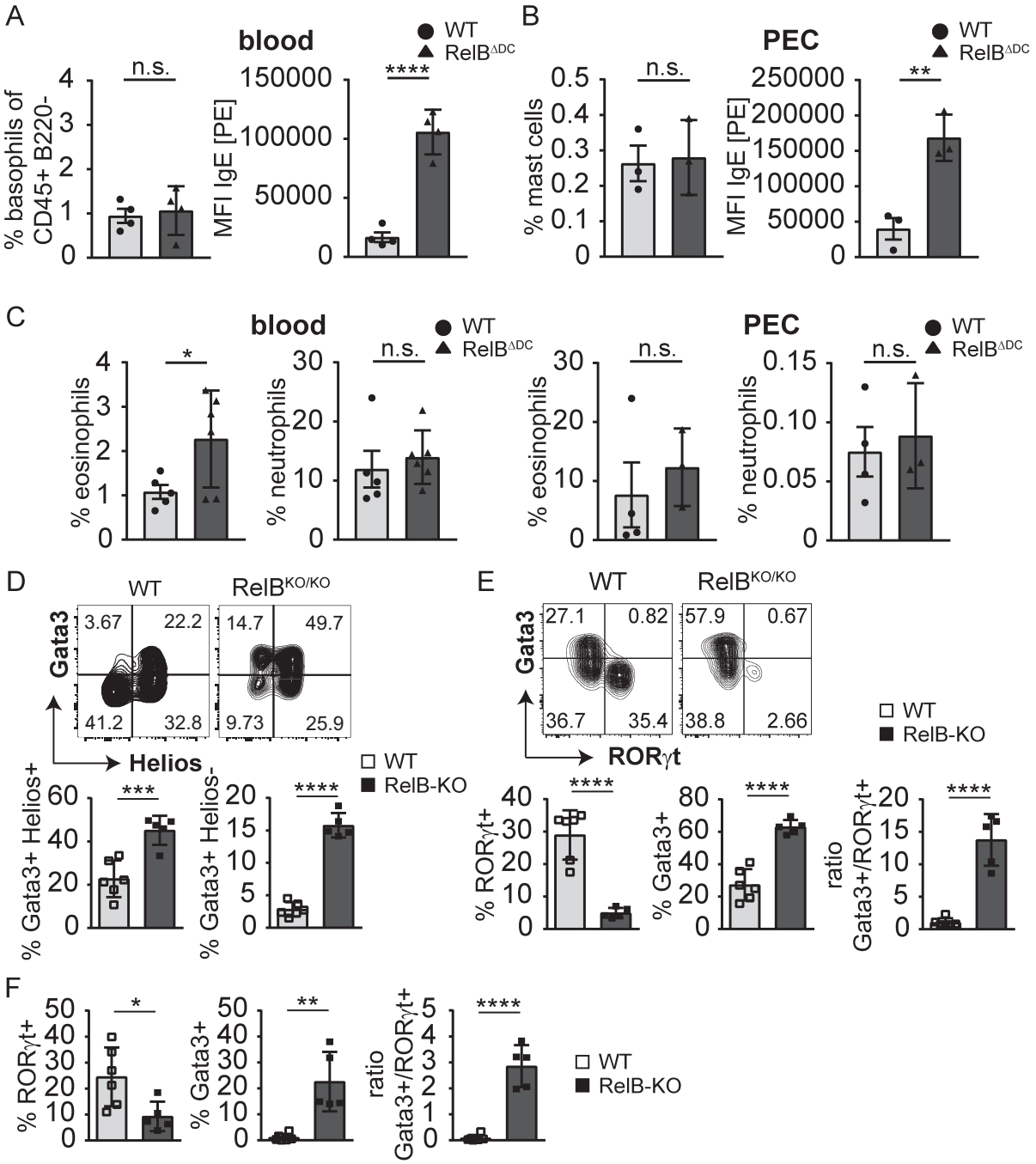

Supplementary Figure 3:

A) Quantification of basophils ($CD49b^+IgE^+$ cells of $CD45^+CD45R^-$) in PBL from control littermates or $RelB^{\Delta DC}$ mice and the MFI of IgE bound on the surface of basophils.

B) Quantification of mast cells ($CD117^+FC\varepsilon R1\alpha^+$ cells of $CD45^+$ cells) in PEC of littermate control or $RelB^{\Delta DC}$ mice and the MFI of IgE bound on the surface of mast cells.

C) Frequencies of eosinophils ($SiglecF^+CD11b^+SSC^{hi}$ cells) and neutrophils ($Ly6G^+Ly6C^-$ cells) of $CD45^+$ cells in PBL of littermate control or $RelB^{\Delta DC}$ mice.

D) Representative FACS plots and quantification of Gata3^{hi}Helios^{+} and Gata3^{hi}Helios^{-} frequencies among pregated Foxp3^{+} Tregs isolated from the lamina propria of the small intestine from RelB-KO mice and wildtype controls.
E) Representative FACS plots, quantification of RORγt and Gata3 expression within pregated Foxp3^{+} Tregs isolated from the lamina propria of the small intestine and ratio between Gata3 and RORγt expressing Tregs from RelB-KO mice or wildtype controls.
F) Frequencies of RORγt^{+} and Gata3^{hi} T cells among Foxp3^{-} T effector cells and ratio between Gata3 and RORγt expressing T effector cells isolated from the small intestine a of RelB-KO mice or wildtype controls.

All data were analyzed by two tailed student's t test. Bar diagrams show mean ± SD. *P<0.05, **P<0.01, ***P<0.001.

Suppl Fig 4

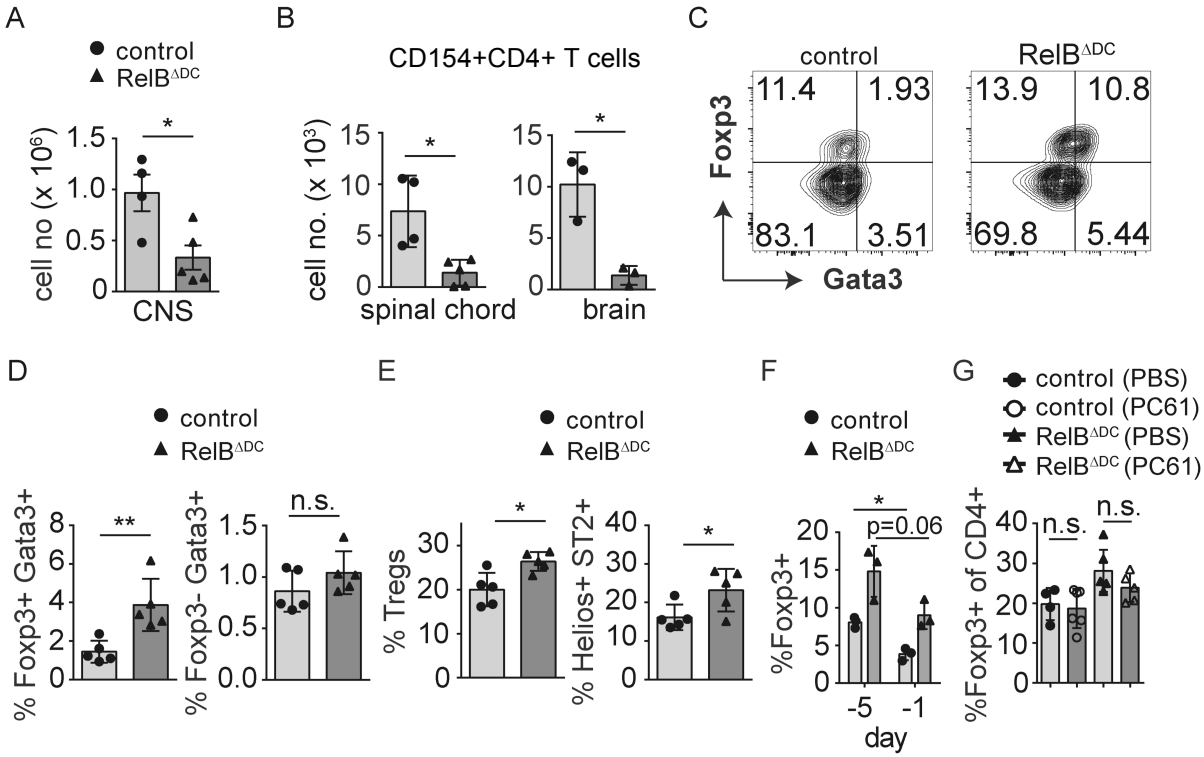

Supplementary Figure 4:

A) Total cell numbers recovered from the CNS at the peak of EAE in littermate control and RelB$^{\Delta DC}$ mice.
B) Total cell numbers of MOG-specific CD154^{+}CD4^{+} T cells in spinal cord and brain in littermate control or RelB$^{\Delta DC}$ mice after restimulation with MOG$_{35-55}$ peptide.
C) Representative FACS plots of Gata3 and Foxp3 expression among CD4^{+} T cells in the CNS at the peak of EAE in littermate control or RelB$^{\Delta DC}$ mice.
D) Quantification of the Gata3^{hi} cell frequencies among Foxp3^{-} and Foxp3^{+} T cells shown in (C).
E) Frequency of Tregs within CD4^{+} T cells or Helios^{+}ST2^{+} cells among Foxp3^{+} Tregs of the inguinal lymph nodes at the peak of EAE in littermate control or RelB$^{\Delta DC}$ mice.
F) Littermate control or RelB$^{\Delta DC}$ mice were treated at day -5 and day -3 with an anti-CD25 depleting antibody (clone PC61) prior to EAE immunization. Percentage of Foxp3^{+} among CD4^{+} T cells in the peripheral blood of littermate control and RelB$^{\Delta DC}$ mice was assessed by flow cytometry at indicated time points prior to immunization.
G) Frequency of Foxp3^{+} cells among CD4^{+} T cells in the CNS after PC61 depletion at the peak of EAE in littermate control or RelB$^{\Delta DC}$ mice.

All data show pooled results of at least two independent experiments and were analyzed by two tailed student's t test. Bar diagrams show mean± SD. *P<0.05, **P<0.01